

1
2
3
4
5
6
7
8
9
10
11
12
13
14
15
16
17
18
19
20
21
22
23
24
25
26
27
28
29
30
31

Seasonal cycles and trends of water budget components in 18 river basins across the Tibetan Plateau: a multiple datasets perspective

Wenbin Liu^a, Fubao Sun^{a,b*}, Yanzhong Li^a, Guoqing Zhang^{b,ec,d},
Yan-Fang Sang^a,
Wee Ho Lim^{a,c}, Jiahong Liu^d, Liu^f, Hong Wang^a, Peng Bai^a

^aKey Laboratory of Water Cycle and Related Land Surface Processes, Institute of Geographic Sciences and Natural Resources Research, Chinese Academy of Sciences, Beijing 100101, China

^bHexi University, Zhangye 734000, China

^b~~Key~~-^c~~Key~~ Laboratory of Tibetan Environmental Changes and Land Surface Processes, Institute of Tibetan Plateau Research, Chinese Academy of Sciences, Beijing 100101, China

^e~~CAS~~-^d~~CAS~~ Center for Excellent in Tibetan Plateau Earth Sciences, Beijing 100101, China

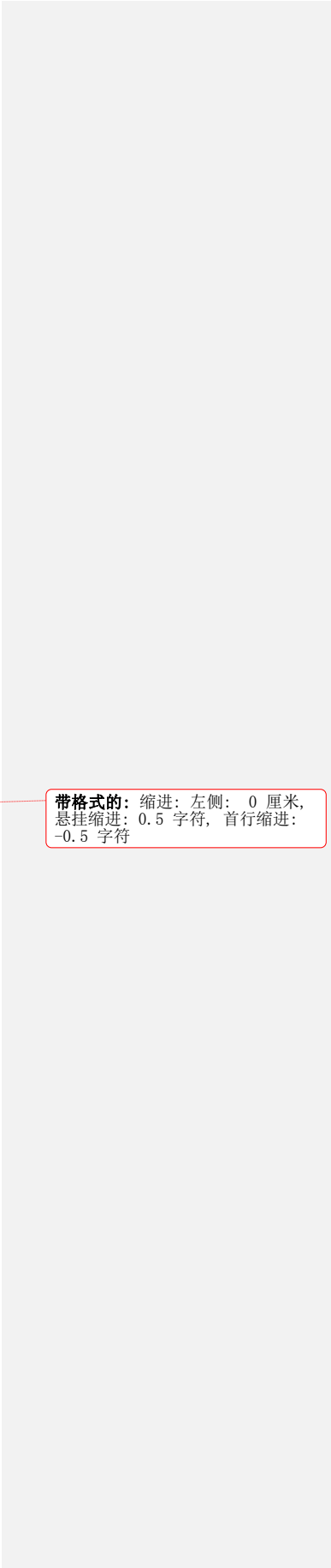
^eEnvironmental Change Institute, Oxford University Centre for the Environment, School of Geography and the Environment, University of Oxford, Oxford OX1 3QY, UK

^d~~Key~~-^f~~Key~~ Laboratory of Simulation and Regulation of Water Cycle in River Basin, China Institute of Water Resources and Hydropower Research, Beijing 100038, China

Submitted to: Hydrology and Earth System Sciences

Corresponding Author: Dr. Fubao Sun (Sunfb@igsnr.ac.cn), from the Key Laboratory of Water Cycle and Related Land Surface Processes, Institute of Geographic Sciences and Natural Resources Research, Chinese Academy of Sciences (No. A11, Datun Road, Chaoyang District, Beijing 100101, China)

Email Addresses for other authors: Wenbin Liu (liuwb@igsnr.ac.cn), Yanzhong Li (liy.14b@igsnr.ac.cn), Guoqing Zhang (guoqing.zhang@itpcas.ac.cn), Yan-fang Sang (sangyf@igsnr.ac.cn), Wee Ho Lim (limwh@igsnr.ac.cn), Jiahong Liu (liujh@iwhr.com), Hong Wang (wanghong@igsnr.ac.cn), Peng Bai (baip.11b@igsnr.ac.cn)



带格式的: 缩进: 左侧: 0 厘米, 悬挂缩进: 0.5 字符, 首行缩进: -0.5 字符

32

33

2017/11/25

带格式的：居中

带格式的：居中，行距：2 倍行距，
无孤行控制，不对齐到网格，制
表位： 33.93 字符，左对齐

34 **Highlights**

- 35 ● ~~Monthly basin wide ET was calculated through water balance considering the~~
36 ~~impacts of glacier and water storage change~~A water balance approach to quantify
37 monthly evapotranspiration which accounts for the changes in glacier and water
38 storage of Tibetan Plateau
- 39 ● ~~Water budget components and trends for 18 river basins over the TP were~~
40 ~~evaluated~~Evaluation of water budget components and trends for 18 river basin in
41 Tibetan Plateau
- 42 ● ~~Uncertainties were discussed from multiple dataset perspective~~Discussion of
43 uncertainties arise from multiple datasets used in Tibetan Plateau

44

45 **Abstract.** The dynamics of water budget over the Tibetan Plateau (TP) are not ~~fully-~~
46 ~~well~~ understood ~~so far due to because of~~ the lack of ~~quantitative observations of the~~
47 ~~land surface water cycle~~ hydroclimatic observations. ~~Here, we investigated the~~
48 ~~seasonal cycles and trends of water budget components, e.g., precipitation, runoff and~~
49 ~~evapotranspiration (ET), in 18 TP basins using multi-source datasets during the period~~
50 ~~1982-2011~~ Based on multi-source datasets over a 30-year period (1982-2011), we
51 investigate the seasonal cycles and trends of water budget components, e.g.,
52 precipitation (P), evapotranspiration (ET) and runoff (Q) of 18 river basins in TP. A
53 ~~two-step bias correction procedure was applied to calculate the basin-wide ET-~~
54 ~~considering the influences of glacier and water storage change~~ We apply a two-step
55 bias-correction procedure to calculate the basin-scale ET considering the changes in
56 glacier and water storage change. The results indicated ~~d~~ that precipitation, which
57 mainly concentrated during June-October (varied among different monsoons impacted
58 basins), is the major contributor to the runoff in the TP basins. The basin-wide snow
59 water equivalent (SWE) was relatively higher ~~er~~ from mid-autumn to spring for ~~most TP~~
60 ~~basins~~ most of the river basins in TP. The water cycles intensified under ~~a~~ global
61 warming in most of these basins; ~~receded in the upper Yellow and Yalong sub-river~~
62 ~~basins due to the~~ except for the upper Yellow and Yalong Rivers, which were
63 ~~significantly influenced by the~~ weakening East Asian monsoon. Consistent with the
64 ~~climate~~ warming climate and moistening in the TP and western China, the aridity
65 index (PET/P) in ~~most basins~~ most of the river basins decreased. These results
66 ~~highlighted-~~ demonstrate the usefulness of integrating the multi-source datasets (e.g.,

67 in situ observations, remote sensing products, reanalysis, land surface model
68 simulations and climate model outputs) for hydrological applications in the
69 data-sparse regions. More generally, such approach might offer helpful insights
70 towards understanding the water/energy budgets and sustainability of water resource
71 management practices of data-sparse regions in a changing environment. ~~—and could—~~
72 ~~be beneficial for understanding the water and energy budgets, sustainable~~
73 ~~management of water resources under a warming climate in the harsh and the~~
74 ~~data sparse Tibetan Plateau.—~~

76 1 Introduction

77 As the highest plateau in the globe (the average elevation is higher than 4000 meters
78 above the sea level), the Tibetan Plateau (TP, also called “the roof of the world” or
79 “the third Pole”) is regarded as one of the most vulnerable region under a warming
80 climate and is ~~subjected~~ exposed to strong interactions among atmosphere,
81 hydrosphere, biosphere and cryosphere in the earth system (Duan and Wu, 2006; Yao
82 et al., 2012; Liu ~~W.~~ et al., 2016b). It ~~also~~ serves as the “Asian water tower” from
83 which ~~many~~ some major Asian rivers such as Yellow ~~river~~ River, Yangtze ~~river~~ River,
84 Brahmaputra ~~river~~ River, Mekong ~~river~~ River, Indus ~~river~~ River, etc., originate. It
85 ~~provides is~~ a vital water resource to support the livelihood of hundreds of millions of
86 people in China and the ~~surrounding neighboring Asian~~ countries (~~Immerzell~~
87 Immerzeel et al., 2010; Zhang et al., 2013). ~~Knowledge about the water budgets and~~
88 ~~their responses to the changing environment is thus crucial for understanding the~~
89 ~~hydrological regimes and for sustainable water resources management as well as~~
90 ~~environmental protection in this special region~~ Hence sound knowledge of water

91 budget and hydrological regimes of TP and its response to changing environment
92 would have practical relevance for achieving sustainable water resource management
93 and environmental protection in this part of the world (Yang et al., 2014; Chen et al.,
94 2015).

95
96 ~~The TP is also known as a typical data sparse mountain region which brings great~~
97 ~~challenges to hydrological and related land surface studies. Despite the importance of~~
98 TP in this geographic region, advance in hydrological and land surfaces studies in this
99 region has been limited by data scarcity (Zhang et al., 2007; Li F. et al., 2013; Liu X.
100 et al., 2016). For ~~example~~ instance, less than 80 observation stations (~10% of a total
101 of ~750 observation station across China) have been established in TP by the ,since
102 ~~the 1950s, totally 750 stations have been established over China by the Chinese~~
103 Meteorological Administration (CMA) since the mid-20th century, among which only
104 less than 80 stations are distributed over the plateau (Wang and Zeng, 2012). These
105 stations are generally sparse and unevenly distributed ~~They are primary sparse and~~
106 ~~unevenly located~~ at relatively low elevation regions, focus only on the meteorological
107 variables and lack of other land surface observations such as evapotranspiration, snow
108 water equivalent and latent heat fluxes, ~~etc.~~ In addition, long-term ~~consecutive~~
109 observations of river discharge, snow depth, lake depth and glacier melts in the TP are
110 also absent (Akhta et al., 2009; Ma et al., 2016). Therefore, ~~the insights of water~~
111 ~~balance over various TP river basins located at different monsoon dominant regions~~
112 ~~are still unclear so far~~ the water balance and hydrological regimes for each river basin
113 of TP and their relation with monsoons are poorly understood (Cuo et al., 2014; Xu et
114 al., 2016). ~~One way to overcome this limitation is to install more instruments to~~
115 ~~measure the in situ water budgets~~ Whilst this shortcoming could be resolved through

带格式的: 上标

116 | installation of in-situ monitoring systems (Yang et al., 2013; Zhou et al., 2013; Ma et
117 | al., 2015), ~~but it is extremely expensive to maintain long term observations at basin or~~
118 | ~~regional scales~~the overall cost of running the operational sites would be substantial.
119 | Another workaround would be through modeling approach, i.e., feeding remote
120 | sensing information and meteorological forcing data into physically-based land
121 | surface model (LSM) to simulate the basin-wide water budget~~is to simulate~~
122 | ~~basin wide water budgets through physical based land surface models at several large~~
123 | ~~river basins forced with remote sensing data and large scale gridded meteorological~~
124 | ~~forcing datasets~~ (Bookhagen and Burbank, 2010; Xue et al., 2013; Zhang et al., 2013;
125 | Cuo et al., 2015; Zhou et al., 2015; Wang et al., 2016). However, such approach is not
126 | immune from the issue of data scarcity at multiple river basins (with varied sizes
127 | and/or terrain complexities) for supporting model calibration and validation purposes
128 | ~~it is still difficult to use land surface models to multiple basins especially to the~~
129 | ~~relatively smaller ones under complex terrains due to the lack of adequate data for~~
130 | ~~model calibration and validation~~ (Li F. et al., 2014).

131 |
132 | Most recently, several ~~A number of~~ global (or regional) datasets relevant to the
133 | calculation of w~~for water budget components~~ have been released ~~recently. They~~
134 | ~~including~~ include remote sensing-based retrievals (Tapley et al., 2004; Zhang et al.,
135 | 2010; Long et al., 2014; Zhang Y. et al., 2016), land surface model (LSM) simulations
136 | (Rui, 2011), reanalysis outputs (Berrisford et al., 2011; Kobayashi et al., 2015) and
137 | gridded forcing data interpolated from the in situ observations (Harries et al., 2014).
138 | For example, there are many products ~~for~~ related to terrestrial evapotranspiration (ET)
139 | such as GLEAM_E (Global Land surface Evaporation: the Amsterdam Methodology,
140 | Miralles et al., 2011a), MTE_E (a product integrated the point-wise ET observation at

141 FLUXNET sites with geospatial information extracted from surface meteorological
142 observations and remote sensing in a machine-learning algorithm, Jung et al., 2010),
143 LSM-simulated ETs from Global Land Data Assimilation System version 2
144 (GLDAS-2) with different land surface schemes (Rodell et al., 2004), ETs from
145 Japanese 55-year reanalysis (JRA55_E), the ERA-Interim global atmospheric
146 reanalysis dataset (ERA-Interim) and the National Aeronautic and Space Administration
147 (NASA) Modern Era Retrospective-analysis for Research and Application (MERRA)
148 reanalysis data (Lucchesi, 2012). Moreover, there are also several global or regional
149 LSM-based runoff simulations from GLDAS and the Variable Infiltration Capacity
150 (VIC) model (Zhang et al., 2014). A few attempts have been made to validate multiple
151 datasets for certain water budget components and to explore their possible
152 hydrological implications. For example, Li X. et al. (2014) and Liu W. et al. (2016a)
153 evaluated multiple ET estimates against the water balance method at annual and
154 monthly time scales. Bai et al. (2016) assessed streamflow simulations of GLDAS
155 LSMs in five major rivers over the TP based on the discharge observations. Although
156 ~~there are certain~~ uncertainties might exist among different datasets with various
157 spatial and temporal resolutions and calculated ~~through using~~ different algorithms
158 (Xia et al., 2012), they offer an opportunity to provide a great chance for us to
159 quantify-examine the general basin-wide water budgets and their uncertainties in
160 gauge-sparse regions such as the TP considered in this study.

161

162 From the multiple datasets perspective, this study aims to investigate the water budget
163 in 18 TP river basins distributed across the Tibetan Plateau; and evaluate seasonal
164 cycles and annual trends of these water budget components. The objectives of this
165 study are (1) to investigate the general water budgets in 18 river basins across the

166 ~~Tibetan Plateau from the perspective of multiple datasets, and (2) to evaluate the~~
167 ~~seasonal cycles and annual trends of water budget components for 18 TP basins. This~~
168 paper is organized as follows: the datasets and methods applied in this study are
169 described in Sect.2. The results of season cycles and annual trends of water budget
170 components for ~~18 TP~~the river basins are presented and discussed in Sect.3. The
171 uncertainties ~~inherited from~~arise from employing multiple datasets are also discussed
172 in the same section. In ~~the~~ Sect.4, we generalize our findings ~~summarized the general~~
173 ~~results~~ which would be helpful for understanding the water balances of the ~~TP Rivers~~
174 ~~located at westerlies dominated, Indian monsoon dominated and East Asian~~
175 ~~monsoon dominated regions~~river basins under constant influence of interplay between
176 westerlies and monsoons (e.g., Indian monsoon, East Asian monsoon) in the Tibetan
177 Plateau.

178

179 **2 Data and ~~Method~~methods**

180 **2.1 Multiple datasets used**

181 **~~2.1.1 Study basins~~**

182 ~~Eighteen river basins over the TP (Fig.1) with the drainage area ranging from 2832 to~~
183 ~~491235 km² (Table 1) are chosen in this study due to the availability of runoff data~~
184 ~~during the period 1982-2011. They mainly locate at the northwestern, southeastern~~
185 ~~and eastern parts of the plateau with multiyear mean and basin averaged temperature~~
186 ~~and precipitation ranging from -5.68 to 0.97 °C and 128 to 717 mm, which are solely~~
187 ~~or combined controlled by the westerlies, the Indian Summer monsoon and the Easter~~
188 ~~Asian monsoon (Yao et al., 2012). The glacier and snow covers are relatively more for~~
189 ~~the westerlies dominant basins such as Yerqiang, Yulongkashi and Keliya~~
190 ~~(10.86-23.27% and 29.16-35.95%, respectively) whereas are less for the East Asian~~

带格式的：两端对齐

191 ~~monsoon dominated basins such as Yellow, Yangtze and Bayin (0.96% and~~
192 ~~9.42–20.05%, respectively) (Table 1).~~

193 ~~<Figure 1, here please, thanks>~~

194 ~~<Table 1, here please, thanks>~~

195 **2.1.2-1** ~~Runoff, Precipitation-precipitation and Terrestrial-terrestrial~~ storage 196 ~~change~~

197 ~~We obtained the o~~Observed daily runoff (Q) ~~of the study period during the period~~
198 ~~1982–2011 was obtained~~ from the National Hydrology Almanac of China (Table 21).

199 There are < 30% missing data in some gauging stations such as Yajiang, Tongren,
200 Gandatan and Zelingou. Therefore, the VIC Retrospective Land Surface Dataset over
201 China (1952~2012, VIC_IGSNRR simulated) with a spatial resolution of 0.25 degree
202 and a daily temporal resolution from the Geographic Sciences and Natural Resources
203 Research (IGSNRR), Chinese Academy of Sciences, is also used. This dataset is
204 derived from the VIC model forced by the gridded daily observed forcing
205 (IGSNRR_forcing) (Zhang et al., 2014). A degree-day scheme was used in the model
206 to ~~consider-account for~~ the influences of snow and glacier on hydrological processes.

207
208 ~~In terms of precipitation (P), we used the gridded monthly precipitation dataset~~
209 ~~available at CMA (spatial resolution of 0.5 degree; 1961-2011; interpolated from~~
210 ~~observations of 2372 national meteorological stations using the Thin Plate Spline~~
211 ~~method) Monthly gridded precipitation dataset (0.5 degree, 1961-2011) from CMA,~~
212 ~~which was interpolated from observations of 2472 national meteorological stations~~
213 ~~using the Thin Plate Spline method, was used in this study (Table 21). Since the~~
214 ~~reliability of this dataset might be restricted by the relatively sparse stations and~~
215 ~~complex terrain conditions of TP, we make an attempt to incorporate two other~~

216 ~~precipitation datasets (IGSNRR forcing and Tropical Rainfall Measuring Mission~~
217 ~~TRMM 3B43 V7). Considering the uncertainty of CMA precipitation over the TP due~~
218 ~~to the relatively sparse stations and the complex terrain conditions, two other~~
219 ~~precipitation datasets (IGSNRR forcing and TRMM (Tropical Rainfall Measuring~~
220 ~~Mission) 3B43 V7, Huffman et al., 2012) were also used.~~ The precipitation from
221 IGSNRR forcing datasets (0.25 degree) was derived by interpolating gauged daily
222 precipitation from 756 CMA stations based on the synergraphic mapping system
223 algorithm (Shepard, 1984; Zhang et al., 2014) and was further bias-corrected using
224 the CMA gridded precipitation.

225 <Table 21, here please, thanks>

226 ~~To get the change in terrestrial storage (ΔS), we used of t~~Three latest global terrestrial
227 water storage anomaly and water storage change (~~ΔS~~) datasets (available on the
228 GRACE Tellus website: <http://grace.jpl.nasa.gov/>) ~~that were~~ retrieved from the
229 Gravity Recovery and Climate Experiment (GRACE, Tapley et al., 2004; Landerer
230 and Swenson, 2012; Long et al., 2014). ~~Briefly, they, which~~ were processed
231 separately at the Jet Propulsion Laboratory (JPL), the GeoForschungsZentrum (GFZ)
232 and the Center for Space Research at the University of Texas (CSR), ~~were used.~~ To
233 minimize the errors and uncertainty of extracted ΔS , we averaged these GRACE
234 retrievals (2002-2013) ~~from three processing centers were averaged and a glacier~~
235 ~~isostatic adjustment correction as well a destriping filter were applied to minimize the~~
236 ~~errors and uncertainties of extracted ΔS .~~ from different processing centers in this study.

237

238 **2.1.3-2 Temperature, potential evaporation and ET**

239 ~~We obtained the~~The CMA monthly gridded temperature dataset (0.5 degree) from
240 CMA; and potential evaporation (PET) dataset (0.5 degree, Harris et al., 2013) from

241 Climatic Research Unit (CRU), ~~in the~~ University of East Anglia, ~~were used in this~~
242 ~~study.~~ Moreover, we used six ~~published~~ global/regional ET products (four diagnostic
243 products and two LSMs simulations, Table 2), namely (1) GLEAM_E (Miralles et al.,
244 2010, 2011), which ~~estimated~~ consist of three sources of ET (transpiration, soil
245 evaporation and interception) ~~separately throughfor~~ bare soil, short vegetation and
246 vegetation with a tall canopy ~~through~~ calculated using a set of algorithm
247 (www.gleam.eu), (2) GNoah_E simulated ~~by using~~ GLDAS-2 with the Catchment
248 Noah scheme (<http://disc.sci.gsfc.nasa.gov/hydrology/data-holdings>) (Rodell et al.,
249 2004), (3) Zhang_E (Zhang et al., 2010), which is estimated using the modified
250 Penman-Monteith ~~approach~~ equation forced with MODIS data, satellite-based
251 vegetation parameters and meteorological observations
252 (<http://www.ntsug.umt.edu/project/et>), (4) MET_E (Jung et al., 2010)
253 (<https://www.bgc-jena.mpg.de/geodb/projects/Home.phs>), (5) VIC_E (Zhang et al.,
254 2014) from VIC_IGSNRR simulations
255 (http://hydro.igsnrr.ac.cn/public/vic_outputs.html) and (6) PML_E (Zhang Y. et al.,
256 2016) computed from global observation-driven Penman-Monteith-Leuning (PML)
257 model (<https://data.csiro.au/dap/landingpage?pid=csiro:17375&v=2&d=true>).

258

259 **2.1.4.3 Vegetation and snow/glacier parameters**

260 To quantify the dynamics of vegetation of each river basin, we applied tThe
261 Normalized Difference Vegetation Index (NDVI) and the Leaf Area Index (LAI) ~~were~~
262 ~~used to quantify the dynamics of vegetation for 18 TP basins~~ (Table 2). Briefly, tThe
263 NDVI data was obtained from the Global Inventory Modeling and Mapping Studies

264 (GIMMS) (Turker et al., 2005)
265 (https://nex.nasa.gov/nex/projects/1349/wiki/general_data_description_and_access/)
266 while the LAI data was collected from the Global Land Surface Satellite (GLASS)
267 products (<http://www.glc.f.umd.edu/data/lai/>) (Liang and Xiao, 2012). ~~Whist the~~
268 ~~change in seasonal snow cover and glacier has significant impact on the water and~~
269 ~~energy budgets of TP, it remains a technical challenge to get reliable observations due~~
270 ~~to harsh environment (especially at the basin scale). However, recently available~~
271 ~~satellite-based/LSM-simulated products might provide adequate characterization of~~
272 ~~the variation of snow cover and glacier. Seasonal snow and glacier are widespread-~~
273 ~~over the plateau which significantly influences the water and energy budgets in the TP,~~
274 ~~but their observations are difficult due to the harsh environment, especially at the~~
275 ~~basin scale. However, there are currently a few satellite based or LSM simulated-~~
276 ~~products which could provide general information about the variations of snow and~~
277 ~~glacier. To quantify the change in snow cover at each basin, we applied the~~ The daily
278 cloud free snow composite product from MODIS Terra-Aqua and the Interactive
279 Multisensor Snow and Ice Mapping System for the Tibetan Plateau ~~was applied to~~
280 ~~quantify the snow cover changes for each basin~~ (Zhang et al., 2012; Yu et al., 2015),
281 ~~in conjunction with t~~ The snow water equivalent (SWE) retrieved from Global Snow
282 Monitoring for Climate Research product (GlobSnow-2, <http://www.globsnow.info/>)
283 and the VIC_IGSNRR simulations ~~were also used in this study~~ (Takala et al., 2011;
284 Zhang et al., 2014). ~~We extracted general distribution of glacier of TP from~~ Moreover,
285 the Second Glacier Inventory Dataset of China ~~was used to extract the general~~
286 ~~distribution of glacier~~ (Guo et al., 2014). All gridded datasets used were first
287 uniformly interpolated to a spatial resolution of 0.5 degree based on the bilinear
288 interpolation to make their inter-comparison possible. The datasets were then

289 extracted for each of TP basins.

290

291 **2.1.5.4 Monsoon indices**

292 ~~In general, t~~The TP climate is ~~generally under the influence of~~~~influenced by~~ the

293 westerlies, Indian summer monsoon and East Asian summer monsoon (Yao et al.,

294 2012). To investigate the changes of monsoon systems and their potential ~~influences-~~

295 ~~impact~~ on the water budget in the TP basins, ~~we used~~ three monsoon indices, namely

296 Asian Zonal Circulation Index (AZCI), Indian Ocean Dipole Mode Index (IODMI)

297 and East Asian Summer Monsoon Index (EASMI), ~~are used in this study.~~ ~~Briefly, t-~~

298 ~~The~~ IODMI is an indicator of the east-west temperature gradient across the tropical

299 Indian Ocean ~~defined by~~ (Saji et al., ~~1999~~), which can be downloaded from the

300 following website:

301 [http://www.jamstec.go.jp/frcgc/research/d1/iod/HTML/Dipole%20Mode%20Index.ht](http://www.jamstec.go.jp/frcgc/research/d1/iod/HTML/Dipole%20Mode%20Index.htm)

302 [m](http://www.jamstec.go.jp/frcgc/research/d1/iod/HTML/Dipole%20Mode%20Index.htm). The EASMI and AZCI (60°-150°E) reflect the dynamics of East Asian summer

303 monsoon (Li and Zeng, 2002) and the westerlies (~~represented by Asian Zonal~~

304 ~~Circulation index~~), which can be obtained from ~~Beijing Normal University (the-~~

305 <http://ljp.gcess.cn/dct/page/65577>) and the National Climate Center of China

306 (<http://ncc.cma.gov.cn/Website/index.php?ChannelID=43WCHID=5>), respectively.

307

308 **2.1.15 Study basins**

309 ~~In this study, we selected 18 river basins of varied sizes (range: 2832-191235 km² ;~~

310 ~~see Table 1 for details) with adequate runoff data over a 30-year period (1982-2011).~~

311 ~~Eighteen river basins over the TP (Fig.1) with the drainage area ranging from 2832 to~~

312 ~~191235 km² (Table 1) are chosen in this study due to the availability of runoff data~~

313 ~~during the period 1982-2011. They are distributed in~~ ~~mainly locate at the northwestern.~~

314 southeastern and eastern parts of the plateau with multiyear-mean and basin-averaged
315 temperature and precipitation ranging from -5.68 to 0.97 °C and 128 to 717 mm,
316 which are solely dominated or under the influences of ~~or combined controlled by the~~
317 westerlies, the Indian Summer monsoon and the Easter Asian monsoon (Yao et al.,
318 2012). ~~There are more~~ The glacier and snow covers are relatively more for in the
319 westerlies-dominant basins such as Yerqiang, Yulongkashi and Keliya (10.86~23.27%
320 and 29.16~35.95%, respectively); less for ~~whereas are less for the East Asian~~
321 monsoon-dominated basins such as Yellow, Yangtze and Bayin (0~0.96% and
322 9.42~20.05%, respectively) (Table ~~1~~2).

323 <Figure 1, here please, thanks>

324 <Table ~~1~~2, here please, thanks>

326 2.2 Methods

327 2.2.1 Water balance-based ET estimation

328 The basin-wide water balance at the monthly and annual timescales could be written
329 as the principle of mass conservation (also known as the continuity equation,

330 Oliveira et al., 2014) of basin-wide precipitation (P, mm), evapotranspiration (ET_{wb},
331 mm), runoff (Q, mm) as well as terrestrial water storage change (ΔS, mm),

$$332 \quad ET_{wb} = P - Q - \Delta S \quad (1)$$

333 In most TP basins, glacier melt (M_G, mm) contributes to river discharge together with
334 precipitation (liquid precipitation and snow). The monthly and annual water balance
335 in these basins can thus be revised as,

$$336 \quad ET_{wb} = P + M_G - Q - \Delta S \quad (2)$$

337 Several attempts have been made for separating glacier contributions to river
338 discharge through site-scale isotopic observations, remote sensing as well as

339 land-surface hydrological modeling for some individual TP basins (Zhang et al., 2013;
340 Zhou et al., 2014; Neckel et al., 2014; Xiang et al., 2016). However, accurate
341 quantification of M_G is difficult in the data-sparse TP, especially for multiple basins.
342 In this study, we simply use the percentages of glacier melt to river discharge for
343 some TP basins derived from the literatures (Chen, 1988; Mansur and Ajjinisa, 2005;
344 Zhang et al., 2013; Liu J. et al., 2016) and the empirical relations between the glacier
345 area ratio (%) and glacier melt in basins mentioned above (Table 3).

346 <Table 33, here please, thanks>

347 The terrestrial water storage (ΔS) in Eq. (2), ~~which~~ includes the surface, subsurface
348 and ground water changes. ~~It has been demonstrated,~~ cannot be neglected in water
349 balance calculation ~~at a over~~ monthly ~~or and~~ annual timescales due to snow
350 ~~accumulation cover change~~ and ~~some~~ anthropogenic interferences ~~such as (e.g.,~~
351 ~~reservoir operation, agricultural water withdrawal) reservoir regulation and~~
352 ~~agriculture irrigation~~ (Liu W. et al., 2016a). ~~For the period 2002-2011, we calculated~~
353 ~~basin-wide The water balance-based ET (ET_{wb}) during 2002-2011 can be calculated~~
354 ~~through directly using the GRACE-derived - Eq. (2) using the GRACE derived mass~~
355 ~~anomaly as ΔS in Eq. (2). Since GRACE data is absent before 2002, we calculated~~
356 ~~the monthly ET_{wb} using the following two-step bias-correction procedure For~~
357 ~~calculation before 2002 when the GRACE data is unavailable, we use a two-step bias~~
358 ~~correction procedure~~ (Li X. et al., 2014) ~~to close the water balance at monthly~~
359 ~~timescale considering the ΔS . We defined $P + M_G - Q$ in Eq. (2) as biased ET~~
360 (ET_{biased} , available from 1982- to 2011) relative to the “true” ET (~~$-ET_{wb} (= P +$~~
361 ~~$M_G - Q - \Delta S_2$ available from during the period 2002-2011 when the GRACE data is~~
362 ~~available) calculated from Eq. (2). Over the period 2002-2011, we first fitted Firstly,~~
363 ~~the ET_{biased} and ET_{wb} series separately over the period 2002-2011 were separately~~

364 fitted using a different gamma distributions, which has been evidenced as an proper
 365 method for modeling the probability distribution of ET (Bouraoui et al., 1999). The
 366 value in monthly ET_{biased} series (2002-2011) can then be bias-corrected through the
 367 inverse function (F^{-1}) of the gamma cumulative distribution function (CDF, F) of
 368 ET_{wb} by matching the cumulative probabilities between two CDFs as follow (Liu ~~W~~
 369 et al., 2016a),

$$ET_{corrected}(m) = F^{-1}(F(ET_{biased}(m)|\alpha_{biased}, \beta_{biased})|\alpha_{wb}, \beta_{wb}) \quad (3)$$

带格式的
带格式的: 行距: 2 倍行距

371 Here α_{biased} , β_{biased} and α_{wb} , β_{wb} are shape and scale parameters of
 372 gamma distributions for ET_{biased} and ET_{wb} . $ET_{corrected}(m)$ and $ET_{biased}(m)$
 373 represent the monthly corrected and biased ET, respectively. The bias correction
 374 procedure can be flexibly applied to the period 1983-2011 by matching the CDF
 375 of ET_{biased} (1983-2011) to that of $ET_{corrected}$ (2002-2011). The second step of
 376 bias correction is to eliminate the annual bias through the ratio of annual
 377 ET_{biased} to annual $ET_{corrected}$ calculated in the first step using the following
 378 method.

带格式的

$$ET_{final}(m) = \frac{ET_{biased}(a)}{ET_{corrected}(a)} \times ET_{corrected}(m) \quad (4)$$

带格式的

380 where $ET_{final}(m)$ is the final monthly ET after bias correction. $ET_{biased}(a)$ and
 381 $ET_{corrected}(a)$ represent the annual biased and corrected ET while
 382 $ET_{corrected}(m)$ is the monthly corrected ET obtained from the first step. The
 383 procedure was then applied to correct the monthly ET_{biased} series and
 384 calculated the monthly $ET_{corrected}$ during the period 1982-2001 for all TP
 385 basins. We take these results as sufficient representation of the "true" ET (ET_{wb})
 386 for evaluating multiple ET products and trend analysis."

带格式的

$$(m) = (F((m)|,)|,)_a \quad (3)$$

带格式的

388 Here, α and β are the shape and scale parameters of gamma distribution for
389 and. The second step is to eliminate the annual bias through the ratio of annual
390 to annual calculated in the first step using the following method,

$$391 \frac{m}{\beta} = \alpha \times (m) \quad (4)$$

392 The procedure was then applied to correct the monthly series and calculated
393 the monthly during the period 1982-2001 for all TP basins. The obtained was
394 seemed as the "true" ET for evaluating multiple ET products and further for the
395 trend analysis.

396 2.2.2 Modified Mann-Kendall test method

397 The Mann-Kendall (MK) test is a rank-based nonparametric approach which is less
398 sensitive to outlier relative to other parametric statistics, but it is sometimes
399 influenced by the serial correlation of time series. Pre-whitening is often used to
400 eliminate the influence of lag-1 autocorrelation before the use of MK test. For
401 example, $X(X_1, X_2, \dots, X_n)$ is a time series data, it in pre-whitening, the analyzed
402 time series $(, , \dots,)$ will be replaced by $(X_2 - cX_1, X_3 - cX_2, \dots, X_{n+1} - cX_n)$ in
403 pre-whitening if the lag-1 autocorrelation coefficient (c) is larger than 0.1 (von Storch,
404 1995). However, significant lag-i autocorrelation may still be detected after
405 pre-whitening because only the lag-1 autocorrelation is considered in pre-whitening
406 (Zhang et al., 2013). Moreover, it sometimes underestimate the trend for a given time
407 series (Yue et al., 2002). Hamed and Rao (1998) proposed a modified version of MK
408 test (MMK) to consider the lag-i autocorrelation and related robustness of the
409 autocorrelation through the use of equivalent sample size, which has been widely used
410 in previous studies during the last five decades (McVicar et al., 2012; Zhang et al.,
411 2013; Liu and Sun, 2016). In the MMK approach, if the lag-i autocorrelation
412 coefficients are significantly distinct from zero, the original variance of MK statistics

带格式的: 字体: Cambria Math

带格式的: 字体: Cambria Math

带格式的: 字体: Cambria Math

带格式的: 字体: Cambria Math,
非加粗

带格式的: 字体: Cambria Math

带格式的: 列出段落

413 will be replaced by the modified one. In this study, we used the MMK approach to
414 quantify the trends of water budget components in 18 TP basins and the significance of
415 trend was tested at the >95% confidence level.

416 3 Results and Discussion

417 3.1 ET evaluation and General hydrological characteristics of 18 TP basins

418 ~~In this study, w~~We first assessed the VIC_IGSNRR simulated runoff against the
419 observations for each basin (for example, at Tangnaihai and Pangduo stations in
420 Fig.2). ~~If the Nash Efficiency coefficient (NSE) between the observation and~~
421 ~~simulation is above 0.65, t~~The VIC_IGSNRR simulated runoff is acceptable and
422 could be used to replace the missing values for a given basin, ~~if the Nash Efficiency-~~
423 ~~coefficient (NSE) between the observation and simulation is above 0.65.~~ Moreover,
424 the CMA precipitation is consistent with TRMM (Corr = 0.86, RMSE = 8.34
425 mm/month) and IGSNRR forcing (Corr = 0.94, RMSE = 7.15mm/month)
426 precipitation for multiple basins (and also for the smallest basin above Tongren station,
427 Fig.2), ~~, although the observation-derived and TRMM-estimated precipitation also has~~
428 ~~uncertainties which reveals the applicability of CMA precipitation under the TP-~~
429 ~~conditions. The magnitudes of GRACE-derived annual mean water storage change~~
430 ~~(ΔS) in 18 TP basins are relatively less than those for other water balance components~~
431 ~~such as annual P, Q and ET (Table 4). The uncertainties among GRACE-derived~~
432 ~~annual mean ΔS from different data processing centers (CSR, GFZ and JPL) are~~
433 ~~small for 18 basins except for in the basins controlled by Gadatan and Tangnaihai~~
434 ~~stations.~~

435

436 < Figure 2, here please, thanks >

437 < Table 4, here please, thanks >

438
439 We then evaluated six ET products in 18 TP basins against our calculated ET_{wb} at a
440 monthly basis during the period 1983-2006 (Fig. 3). The ranges of monthly averaged
441 ET among different basins (approximately 4–39 mm month⁻¹) are very close for all
442 products compare ~~with~~to that calculated from the ET_{wb} (6–42 mm month⁻¹). However,
443 GLEAM_E (correlation coefficient: Corr = 0.85 and root-mean-square-error: RMSE =
444 5.69 mm month⁻¹) and VIC_E (Corr = 0.82 and RMSE = 6.16 mm month⁻¹) perform
445 relatively better than others. Although Zhang_E and GNoah_E were found closely
446 correlated to monthly ET_{wb} in the upper Yellow River, the upper Yangtze River,
447 Qiangtang and Qaidam basins (Li X. et al., 2014), they did not exhibit overall good
448 performances (Corr = 0.61, RMSE = 7.97 mm month⁻¹ for Zhang_E and Corr = 0.42,
449 RMSE = 10.16 mm month⁻¹ for GNoah_E) for 18 TP basin used in this study. We thus
450 use GLEAM_E and VIC_E together with ET_{wb} to calculate the seasonal cycles and
451 trends of ET in 18 TP basins in the following sections.

452 [< Figure 3, here please, thanks >](#)

453 To investigate the general hydroclimatic characteristics of rivers over the TP, we
454 classify 18 basins into three categories, namely westerlies-dominated basins
455 (Yerqiang, Yulongkashi and Kelia), Indian monsoon-dominated basins (Brahmaputra
456 and Salween), and East Asian monsoon-dominated basins (Yellow, Yalong and
457 Yangtze) referred to Tian et al. (2007), Yao et al. (2012) and Dong et al. (2016).
458 Interestingly, they are clustered into three groups under Budyko framework (Budyko,
459 1974; Zhang D. et al., 2016) with relatively lower evaporative index ~~for~~in Indian
460 monsoon-dominant basins and higher aridity index ~~for~~in westerlies-dominant basins,
461 which reveal various long-term hydroclimatologic conditions (Fig. 4). Overall, the
462 annual mean air temperature increases (-5.68 ~0.97 °C) while multiyear mean glacier

463 area (and thus the glacier melt normalized by precipitation) decreases (23.27 ~ 0%)
464 gradually from the westerlies-dominant, Indian monsoon-dominant to East Asian
465 monsoon-dominant basins. The vegetation status (NDVI range: 0.05~0.43; LAI range:
466 0.03~0.83) tends to be better and ET increases (and thus runoff coefficient gradually
467 decreases) from cold to warm basins (Fig. 4 and Table 1). The R^2 between
468 basin-averaged NDVI and ET is 0.76 which shows a clear vegetation control on ET in
469 18 TP basins. The results ~~is-are~~ in line with Shen et al. (2015), which indicated that
470 the spatial pattern of ET trend was significantly and positively correlated with NDVI
471 trend over the TP. The dominant climate systems are overall discrepant for the three
472 TP regions with different water-energy characteristics and sources of water vapor. The
473 westerlies-controlled basins are relatively colder than the Indian monsoon-dominated
474 basins, thus they develop more glaciers (and thus have more snow melt contributions
475 to total river streamflow) and have relatively less vegetation (and thus limit vegetation
476 transpiration). It is a general picture of hydrological regime in high-altitude and cold
477 regions (Zhang et al., 2013; Cuo et al., 2014), which could be interpreted from the
478 perspective of multi-source datasets in the data-sparse TP.

479 < Figure 4, here please, thanks >

480 3.2 Seasonal cycles of basin-wide water budget components for the TP basins

481 The multi-year means of water budget components (i.e., P, Q, ET, snow cover and
482 SWE) and vegetation parameters (i.e., NDVI and LAI) ~~were-are~~ calculated for each
483 calendar month and for 18 TP river basins using multi-source datasets available from
484 1982 to 2011. Overall, the seasonal variations of P, Q, ET, air temperature and
485 vegetation parameters are similar in all TP basins with peak values occurred in May to
486 September (Fig.5 and Fig.6). The seasonal cycles of snow cover and SWE are
487 generally ~~time~~ consistent among the as well for 18 TP basins (the peak values mainly

488 occur from October to next April, Fig.7). With the ascending air temperature from
489 cold to warm months, the basin-wide precipitation increases and vegetation cover
490 expandsturns green gradually (the basin-wide ET also increase). Meanwhile, snow
491 cover and glaciers retreat and snow melt or vanish gradually with the melt water
492 supplying the river discharge together with precipitation. The inter-basin variations of
493 hydrological regime are to a large extent linked to the climate systems that prevail
494 over the TP.

495 < Figure 5, here please, thanks >

496 Although the temporal patterns of hydrological components are generally analogous,
497 they varied-vary among the parameters, climate zones and even basins (Zhou et al.,
498 2005). For example, relative to air temperature, the seasonal pattern of variation of
499 runoff is more-similar to precipitation which reveals that runoff is mainly controlled
500 by precipitation in most TP basins. It is in agreement with that summarized by Cuo et
501 al. (2014). In the westerlies-dominated basins, the peak values of precipitation and
502 runoff mainly concentrate in June-August, which contribute approximately 68-82%
503 and 67-78% of annual totals, respectively. During this period, the runoff always
504 exceeds precipitation which indicates large contributions of glacier/snow-melt water
505 to streamflow. It is consistent with the existing findings in Tarim River (Yerqiang,
506 Yulongkashi and Keliya rivers are the major tributaries of Tarim River), which
507 indicated that the melt water accounted for about half of the annual total streamflow
508 (Fu et al., 2008). The ET (vegetation cover) in three westerlies-dominated basins are
509 relatively less (scarcer) than that in other TP basins while the percentages of glacier
510 and seasonal snow cover are higher in these basins which contribute more melt water
511 to river discharge (Fig.6 and Fig.7). Overall, the SWE in Yerqiang, Yulongkashi and
512 Keliya rivers are relatively-higher in winter than other seasons, but they vary with

513 | basins and products which ~~reveal~~reflect considerable uncertainties in SWE
514 | estimations.

515 | [< Figure 6, here please, thanks >](#)

516 | In the Indian monsoon and East Asian monsoon-dominated basins, the runoff
517 | concentrates during June-September (or June- October) with precipitation being the
518 | dominant contributor of annual total runoff. For example, the peak values of
519 | precipitation and runoff occur during June-September at Zhimenda station
520 | (contributing about 80% and 74% of the annual totals) while those occur during
521 | June-October at Tangnaihahi station (contributing about 78% and 71% of the annual
522 | totals, respectively). The results are quite similar to the related studies in eastern and
523 | southern TP such as Liu (1999), Dong et al. (2007), Zhu et al. (2011), Zhang et al.
524 | (2013), Cuo et al. (2014). The vegetation cover (ET) in most basins is ~~relatively better~~
525 | denser (higher) than that in the westerlies-dominant basins. Moreover, the seasonal
526 | snow mainly covers from mid-autumn to spring and correspondingly the SWE is
527 | relatively higher in these months in all basins except for Yellow River above Xining
528 | station, Salween River above Jiayuqiao station and Brahmaputra River above Nuxia
529 | and Yangcun stations.

530 | [< Figure 7, here please, thanks >](#)

531 | **3.3 Trends of basin-wide water budget components for the TP basins**

532 | ~~Trends in water budget components for 18 TP basins during the period 1982-2011~~
533 | ~~were also examined through the modified Mann-Kendall test (MMK) in this study.~~
534 | The hydrological cycles has intensified in the westerlies-dominated basins with Q, P
535 | and ET_{wb} all ascended ~~with~~under regional warming (Fig.8), especially in the Keliya
536 | River basin (Numaitilangan station). The aridity index (PET/P), which is an indicator
537 | for the degree of dryness, slightly declined in all basins in northwestern TP. Although

538 | ~~both~~ P and PET were found ~~both~~ increase since the 1980s (Shi et al., 2003; Yao et al.,
539 | 2014), the declined PET/P is, to some extent, attributed to the ascending P exceed the
540 | increase in PET ~~for in~~ these basins (except for the Yulongkashi basin). ~~_~~The climate
541 | moistening ([Shi et al., 2003](#)) in the headwaters of these inland rivers would be
542 | beneficial to the water resources and oasis agro-ecosystems in the middle and lower
543 | basins. The increase in streamflow was also found in most tributaries of the Tarim
544 | River (Sun et al., 2006; Fu et al., 2010; Mamat et al., 2010).

545 |
546 | Moreover, the westerlies, revealed by the Asian Zonal Circulation Index (60°-150° E),
547 | slightly enhanced (linear trend: 0.21) over the period ~~of~~ 1982-2011 (Fig.9). ~~With the~~
548 | ~~strengthening westerlies, more~~More water vapor ~~was may be~~ transported and fell as
549 | precipitation or snow in northwestern TP (e.g., the eastern Pamir region) ~~with the~~
550 | ~~strengthening westerlies~~. Both SWE products (VIC_IGSNRR simulated and
551 | GlobaSnow-2 product) showed slightly ~~_~~ increase ~~for across~~ all basins with ~~the~~
552 | ~~incremental~~rising seasonal snow covers and ~~advanced~~ glaciers (Yao et al., 2012).
553 | More precipitation was transformed into snow or glacier and the runoff coefficient
554 | (Q/P) exhibited decrease although precipitation obviously increased (Fig.8). In
555 | addition, the transpiration in these basins ~~may might~~ decrease with vegetation
556 | degradation ~~as~~ revealed by the NDVI and LAI (Yin et al., 2016) but the atmospheric
557 | evaporative demand indicated by CRU PET increased (significantly increase in the
558 | Yulongkashi and Keliya rivers) during the period 1982-2011.

559 | [< Figure 8, here please, thanks >](#)

560 | [< Figure 9, here please, thanks >](#)

561 | In the East Asian monsoon-dominated basins, there are two types of change for
562 | basin-wide water budget components. For example, P and Q slightly decreased in the

563 upper Yellow River (Tangnihai, Huangheyuan and Jimai stations) and Yalong River
564 (Yajiang station) but increased in other basins (Zelingou, Gandatan, Xining, Tongren
565 and Zhimenda stations) over the period of 1982-2011 (Fig.10). The decline in Q and P
566 for the upper Yellow and Yalong Rivers (locate at the eastern Tibetan Plateau) were
567 consistent with that found by Cuo et al. (2013, 2014) as well as Yang et al. (2014), and
568 were in line with the weakening (linear slope: -0.01) of the East Asian Summer
569 Monsoon (Fig.9). The vegetation turned green while ET_{wb} and PET increased in all
570 nine basins with the significantly ascending air temperature during the period
571 1982-2011. The aridity index (PET/P) ~~was found~~ decreased in all basins except for the
572 upper Yellow River basin above Jimai station and the upper Yalong River basin above
573 Yajiang station. Moreover, both the runoff coefficients and SWE ~~were~~ decreased
574 except for the Bayin River above Zelingou station and the upper Yellow River above
575 Tongren station in the East Asian monsoon dominated basins.

576 < Figure 10, here please, thanks >

577 The hydrological cycles ~~were also found~~ intensified in the Indian monsoon-dominated
578 basins such as Salween River and Brahmaputra River (Fig.11), ~~which were~~ in line
579 with the strengthening (linear trend: 0.01) of the Indian ~~Summersummer~~ monsoon
580 (revealed by the Indian Ocean Dipole Mode Index) during the specific period
581 1982-2011 (Fig.9). In the six basins, trends in P, Q and ET_{wb} ~~were~~ are all upward.
582 For example, at Jiayuqiao station, the annual streamflow showed slightly increasing
583 trend which was consistent with that examined during 1980-2000 by Yao et al. (2012).
584 The vegetation status, revealed by NDVI and LAI, turned better ~~significantly~~ with the
585 ascending air temperature. The aridity index (PET/P) decreased in all basins except
586 for the Brahmaputra River above Tangjia station, which indicated that most basins in
587 the Indian monsoon-dominated regions turn wet over the period of 1982-2011. The

588 runoff coefficient (Q/P) increased at Gongbujiangda and Nuxia while decreased at
589 Jiayuqiao, Pangduo, Tangji and Yangcun stations. Moreover, the basin-wide SWE
590 declined in the upper Salween River and Brahmaputra River above Pangduo, Tangjia
591 and Gongbujiangda stations while increased in Brahmaputra River above Nuxia and
592 Yangcun stations.

593 < Figure 11, here please, thanks >

594 3.4 Uncertainties

595 The results may unavoidably associate with several aspects of uncertainties ~~which-~~
596 ~~mainly~~-inherited from the multi-source datasets ~~used~~. For example, although the
597 seasonal cycles of ET_{wb} can be captured by GLEAM_E and VIC_E, they still have
598 considerable uncertainties ~~such as~~ at some stations (e.g., Numaitilangan,
599 Gongbujiangda and Nuxia-stations) (Fig.5). ~~With respect to~~ Compared to the the-
600 annual trend of ET_{wb} (Table 4), most ET products (including the well-performed
601 GLEAM_E and VIC_E in some basins) cannot detect the decreasing trends in 7 out of
602 18 basins (at Kulukelangan, Tongguziluoke, Xining, Tongren, Jimai, Nuxia and
603 Gongbujiangda stations) due to their different forcing data; algorithm used as well as
604 varied spatial-temporal resolutions (Xue et al., 2013; Li et al., 2014; Liu W et al.,
605 2016a). In particular, it is well known that land surface models have some difficulties
606 (e.g., parameter tuning in boundary layer schemes) when applying to the TP, even
607 though they have good performances in different regimes (Xia et al., 2012; Bai et al.,
608 2016). For example, Xue et al. (2013) indicated that GNoah E underestimated
609 the ET_{wb} in the upper Yellow River and Yangtze River basins on the Tibetan Plateau
610 mainly due to its negative-biased precipitation forcing. We thus only used ET_{wb} in
611 the trend detection of water budget components in Fig.8, Fig.10 and Fig.11 in this
612 study.

带格式的: 字体: 小四, 非加粗,
非倾斜, 字体颜色: 文字 1

带格式的: 字体: 小四, 非加粗,
非倾斜, 字体颜色: 文字 1

613 The two SWE products also showed large uncertainty with respect to both their
614 seasonal cycles and trends. The VIC_IGSNRR simulated and GlobaSnow-2 SWEs
615 have not been validated in the TP due to the lack of snow water equivalent
616 observations, but in some basins (e.g., Zelingou and Numaitilangan) they showed
617 similar seasonal cycles and annual trends.

618

619

620

621

622

623 Moreover, the interpolation of missing values of runoff with VIC_IGSNRR simulated

624 runoff and the gridded precipitation data (which interpolated from limited gauged

625 precipitation over the plateau) ~~also involved introduced some uncertainties as well as.~~

626 There are also considerable uncertainties arising from empirical extending the ET

627 series back prior to the GRACE era. Finally, we obtained the contributions of

628 glacier-melt to discharge in some basins from the literatures and took them as ~~fixed~~

629 constant numbers. It may inherit considerable uncertainty from varied studies using

630 different approaches such as glacier mass-balance observation, isotope observation

631 and hydrological modeling, and the contribution rates would also change under a

632 warming climate. However, ~~accurate-reliable~~ quantification of the contribution of

633 glacier-melt to discharge is technically ~~difficult nowadays challenging~~, especially for

634 the data-sparse basins. With these caveats, we can interpret the general hydrological

635 regimes and their responses to the changing climate in the TP basins from solely the

636 perspective of multi-source datasets, which are comparable to the existing studies

637 based on the in situ observations and complex hydrological modeling.

<Table 45, here please, thanks>

4 Summary

In this study, we investigated the seasonal cycles and trends of water budget components in 18 TP basins during the period 1982-2011, which is not well understood so far due to the lack of adequate observations in the harsh environment, through integrating the multi-source global/regional datasets such as gauge data, satellite remote sensing and land surface model simulations. By using a two-step bias correction procedure, we calculated the annual basin-wide ET_{wb} ~~was calculated~~ through the water balance approach considering the impacts of glacier and water storage change. ~~The~~ We found that the GLEAM_E and VIC_E ~~were found~~ perform better relative to other products against the calculated ET_{wb} .

From the Budyko framework perspective, ~~t~~the general water and energy budgets ~~were~~ are different in the westerlies-dominated (with higher aridity index, runoff coefficient and glacier cover), the Indian monsoon-dominated and the East Asian monsoon-dominated (with higher air temperature, vegetation cover and evapotranspiration) basins ~~under the perspective of Budyko framework~~. In the 18 TP basins, precipitation is the major contributor to the river runoff, which concentrates mainly during June-October (June-August for the westerlies-dominated basins, June-September or June to October for the Indian monsoon-dominated and the East Asian monsoon-dominated basins). The basin-wide SWE is relatively higher from mid-autumn to spring for all 18 TP basins except for Keliya River and Brahmaputra River above the Nuxia and Yangcun stations. The vegetation cover is relatively less whereas snow/glacier cover is more in the westerlies-dominant basins compared ~~with~~ to other basins. In the period 1982-2011, we found that hydrologic cycle intensified

663 | ~~across most of the basins in Tibetan Plateau; receded at some tributaries located at the~~
664 | ~~upper Yellow River and Yalong River (due to weakening East Asian monsoon). The~~
665 | ~~hydrological cycles were found intensified under the regional warming in most TP~~
666 | ~~basins except for most tributaries of the upper Yellow River and the Yalong River,~~
667 | ~~which were significantly influenced by the weakening East Asian monsoon during the~~
668 | ~~period 1982-2011.~~ The aridity index (PET/P) exhibited decrease in most TP basins
669 | which corresponded to the warming and moistening climate in the TP and western
670 | China. Moreover, the runoff coefficient (Q/P) declined in most basins which may be,
671 | to some extent, due to ET increase induced by vegetation greening and the influences
672 | of snow and glacier changes. Although there are considerable uncertainties inherited
673 | from multi-source data used, the general hydrological regimes in the TP basins could
674 | be revealed, which are consistent to the existing results obtained from in situ
675 | observations and complex land surface modeling. It indicated the usefulness of
676 | integrating the multiple datasets ~~available (e.g., such as~~ in situ observations, remote
677 | sensing-based products, reanalysis outputs, land surface model simulations and
678 | climate model outputs) for hydrological applications. The ~~generalization here results-~~
679 | ~~obtained~~ could be helpful for understanding the hydrological cycles and supporting
680 | sustainable ~~-further for the~~ water resources management and eco-environment
681 | protection ~~under a warming climate~~ in the ~~vulnerable~~ Tibetan Plateau under global
682 | warming.

683

684 | **Author contributions.** Wenbin Liu and Fubao Sun developed the idea to see the
685 | general water budgets in the TP basins from the perspective of multisource datasets.
686 | Wenbin Liu collected and processed the multiple datasets with the help of Yanzhong
687 | Li, Guoqing Zhang, Wee Ho Lim, Hong Wang as well as Peng Bai, and prepared the

688 manuscript. The results were extensively commented and discussed by Fubao Sun,
689 Jiahong Liu and Yan-Fang Sang.

690

691 **Acknowledgements.** This study was supported by the National Key Research and
692 Development Program of China (2016YFC0401401 and 2016YFA0602402), National
693 Natural Science Foundation of China (41401037 and 41330529), the Open Research
694 Fund of State Key Laboratory of Desert and Oasis Ecology in Xinjiang Institute of
695 Ecology and Geography, Chinese Academy of Sciences (CAS), the CAS Pioneer
696 Hundred Talents Program (Fubao Sun), ~~the Initial Founding of Scientific Research~~
697 ~~(Y5V50019YE) and, the CAS President's International Fellowship Initiative~~
698 ~~(2017PC0068) and~~ the program for the "Bingwei" Excellent Talents from the Institute
699 of Geographic Sciences and Natural Resources Research, CAS. We are grateful to the
700 NASA MEaSUREs Program (Sean Swenson) for providing the GRACE land data
701 processing algorithm. The basin-wide water budget series in the TP Rivers used in this
702 study are available from the authors upon request (liuwb@igsnr.ac.cn). We ~~wish to~~
703 thank the editors and reviewers for their invaluable comments and constructive
704 suggestions ~~to improve the quality of the manuscript.~~

705

706 **References**

- 707 Akhtar, M., Ahmad, N., and Booij, M.J.: Use of regional climate model simulations as input for
708 hydrological models for the Hindukush-Karakorum-Himalaya region, Hydrol. Earth Syst. Sci.
709 13, 1075-1089, 2009.
- 710 Bai, P., Liu, X.M., Yang, T.T., Liang, K., and Liu, C.M.: Evaluation of streamflow simulation
711 results of land surface models in GLDAS on the Tibetan Plateau, J. Geophys. Res. Atmos., 121,
712 12180-12197, 2016.
- 713 Berrisford, P, Lee, D., Poli, P., Brugge, R., Fielding, K., Fuentes, M., Kallberg, P., Kobayashi, S.,

714 Uppala, S., and Simmons, A.: The ERA-interim archive. ERA Reports Series No. 1 Version 2.0,
715 Available from: <[https://www.researchgate.net/publication/41571692_The_ERA-interim](https://www.researchgate.net/publication/41571692_The_ERA-interim_archive)
716 archive>, 2011.

717 Bookhagen, B. and Burbank, D.W.: Toward a complete Himalayan hydrological budget:
718 spatiotemporal distribution of snowmelt and rainfall and their impact on river discharge, *J.*
719 *Geophys. Res.*, 115, F03019, 2010.

720 Bouraoui, F., Vachaud, G., Li, L.Z.X., LeTreut, H., and Chen, T.: Evaluation of the impact of
721 climate changes on water storage and groundwater recharge at the watershed scale, *Clim. Dyn.*,
722 15(2), 153-161, 1999.

723 Budyko, M.I.: *Climate and life*. Academic Press, 1974.

724 Chen, D., Xu, B., Yao, T., Guo, Z., Cui, P., Chen, F., Zhang, R., Zhang, X., Zhang, Y., Fan, J., Hou,
725 Z., and Zhang, T.: Assessment of past, present and future environmental changes on the Tibetan
726 Plateau, *Chinese SCI. Bull.*, 60(32), 3025-3035, 2015 (in Chinese).

727 Chen, J.: Lichenometrical studies on glacier changes during the Holocene Epoch at the sources
728 region of Urumqi River, *Sci. China B.*, 18(1), 95-104, 1988 (in Chinese).

729 Cuo, L., Zhang, Y.X., Bohn, T.J., Zhao, L., Li, J.L., Liu, Q.M., and Zhou, B.R.: Frozen soil
730 degradation and its effects on surface hydrology in the northern Tibetan Plateau, *J. Geophys.*
731 *Res. Atmos.*, 120(6), 8276-8298, 2015.

732 Cuo, L., Zhang, Y.X., Gao, Y., Hao, Z., and Cairang, L.: The impacts of climate change and land
733 cover/use transition on the hydrology in the upper Yellow River Basin, China, *J. Hydrol.*, 502,
734 37-52, 2013.

735 Cuo, L., Zhang, Y.X., Zhu, F.X., and Liang, L.Q.: Characteristics and changes of streamflow on
736 the Tibetan Plateau: A review, *J. Hydrol. Reg. stud.*, 2, 49-68, 2014.

737 Dong, X., Yao, Z., and Chen, C.: Runoff variation and responses to precipitation in the source
738 regions of the Yellow River, *Resour. Sci.*, 29(3), 67-73, 2007 (in Chinese).

739 Dong, W., Lin, Y., Wright, J.S., Ming, Y., Xie, Y., Wang, B., Luo, Y., Huang, W., Huang, J., Wang,
740 L., Tian, L., Peng, Y., and Xu, F.: Summer rainfall over the southwestern Tibetan Plateau
741 controlled by deep convection over the Indian Subcontinent, *Nat. Commun.*, 7, 10925, 2016.

742 Duan, A.M. and Wu, G.X.: Change of cloud amount and the climate warming on the Tibetan
743 Plateau, *Geophys. Res. Lett.*, 33, L22704, 2006.

744 Fu, L., Chen, Y., Li, W., Xu, C., and He, B.: Influence of climate change on runoff and water
745 resources in the headwaters of the Tarim River, *Arid Land Geogr.*, 31(2), 237-242, 2008 (in
746 Chinese).

747 Fu, L., Chen, Y., Li, W., He, B., and Xu, C.: Relation between climate change and runoff volume
748 in the headwaters of the Tarim River during the last 50 years., *J. Desert Res.*, 30(1), 204-209,
749 2010 (in Chinese).

750 Guo, W.Q., Liu, S.Y., Yao, X.J., Xu, J.L., Shangguan, D.H., Wu, L.Z., Zhao, J.D., Liu, Q., Jiang,
751 Z.L., Wei, J.F., Bao, E.J., Yu, P.C., Ding, L.F., Li, G., Ge, C.M., and Wang, Y.: The Second
752 Glacier Inventory Dataset of China, Cold and Arid Regions Science Data Center at Lanzhou,
753 doi: 10.3972/glacier.001.2013.db, 2014.

754 Hamed, K.H. and Rao, A.R.: A modified Mann-Kendall trend test for autocorrelation data,
755 *J.Hydrol.*, 204(1-4), 182-196, 1998.

756 Huffman, G.J., , E.F., Bolvin, D.T., Nelkin, E.J., and Adler, R.F.: last updated 2013: TRMM
757 Version 7 3B42 and 3B43 Data Sets, NASA/GSFC, Greenbelt, MD. Data set accessed at
758 [http://mirador.gsfc.nasa.gov/cgi-bin/mirador/](http://mirador.gsfc.nasa.gov/cgi-bin/mirador/presentNavigation.pl?tree=project&project=TRMM&dataGroup=Gridded&CGIS)
759 [presentNavigation.pl?tree=project&project=TRMM&dataGroup=Gridded&CGIS](http://mirador.gsfc.nasa.gov/cgi-bin/mirador/presentNavigation.pl?tree=project&project=TRMM&dataGroup=Gridded&CGIS)
760 [ESSID=5d12e2ffa38ca2aac6262202a79d882a](http://mirador.gsfc.nasa.gov/cgi-bin/mirador/presentNavigation.pl?tree=project&project=TRMM&dataGroup=Gridded&CGIS), 2012.

761 Harris, I., Jones, P.D., Osborn, T.J., and Lister, D.H.: Updated high-resolution grids of monthly
762 climatic observations – the CRU TS3.10 Dataset, *Int. J. Climatol.*, 34 (3), 623-642, 2014.

763 Immerzeel, W.W., van Beek, L.P.H., and Bierkens, M.F.P.: Climate change will affect the Asian
764 water towers, *Science*, 328, 1382-1385, 2010.

765 Jung, M., Reichstein, M., Ciais, P., Seneviratne, S.I., Sheffield, J., Goulden, M.L., Bonan, G.,
766 Cescatti, A., Chen, J., de Jeu, R., Dolman, A.J., Eugster, W., Gerten, D., Gianelle, D., Gobron, N.,
767 Heinke, J., Kimball, J., Law, B.E., Montagnani, L., Mu, Q., Mueller, B., Oleson, K., Papale, D.,
768 Richardson, A.D., Rouspard, O., Running, S., Tomelleri, E., Viovy, N., Weber, U., Williams, C.,
769 Wood, E., Zaehle, S., and Zhang, K.: Recent decline in the global land evapotranspiration trend
770 due to limited moisture supply, *Nature*, 467, 951-954, 2010.

771 Kobayashi, S., Ota, Y., Harada, Y., Ebita, A., Moriya, M., Onoda, H., Onogi, K., kamahori, H.,

772 kobayashi, C., Endo, H., miyaoka, K., and Takahashi, K.: The JRA-55 Reanalysis: General
773 specifications and basic characteristics, *J.Meteor. Soc. Japan*, 93(1), 5-58, doi:
774 10.2151/jmsj.2015-001, 2015.

775 Landerer, F.W. and Swenson, S.C.: Accuracy of scaled GRACE terrestrial water storage estimates,
776 *Water Resour.Res.*, 48, W04531, 2012.

777 Li, F.P., Zhang, Y.Q., Xu, Z.X., Liu, C.M., Zhou, Y.C., and Liu, W.F.: Runoff predictions in
778 ungauged catchments in southeast Tibetan Plateau, *J. Hydrol.*, 511, 28-38, 2014.

779 Li, F.P., Zhang, Y.Q., Xu, Z.X., Teng, J., Liu, C.M., Liu, W.F., and Mpelasoka, F.: The impact of
780 climate change on runoff in the southeastern Tibetan Plateau, *J. Hydrol.*, 505, 188-201, 2013.

781 Li, J.P. and Zeng, Q.C.: A unified monsoon index, *Geophy. Res. Lett.*, 29(8), 1274, 2002.

782 Li, X.P., Wang, L., Chen, D.L., Yang, K., and Wang, A.H.: Seasonal evapotranspiration changes
783 (1983-2006) of four large basins on the Tibetan Plateau, *J. Geophys. Res.*, 119 (23),
784 13079-13095, 2014.

785 Liang, S.L. and Xiao, Z.Q.: Global Land Surface Products: Leaf Area Index Product Data
786 Collection(1985-2010), Beijing Normal University, doi:10.6050/glass863.3004.db, 2012.

787 Liu, J., Liu, T., Bao, A., De Maeyer, P., Feng, X., Miller, S.N., and Chen, X.: Assessment of
788 different modeling studies on the spatial hydrological processes in an arid alpine catchment,
789 *Water Resour. Manag.*, 30, 1757-1770, 2016.

790 Liu, T.: Hydrological characteristics of Yalungzangbo River, *Acta Geogr. Sin.*, 54 (Suppl.),
791 157-164, 1999 (in Chinese).

792 Liu, W.B. and Sun, F.B.: Assessing estimates of evaporative demand in climate models using
793 observed pan evaporation over China, *J. Geophys. Res. Atmos.*, 121, 8329-8349, 2016.

794 Liu, W.B., Wang, L., Zhou, J., Li, Y.Z., Sun, F.B., Fu, G.B., Li, X.P., and Sang, Y-F.: A worldwide
795 evaluation of basin-scale evapotranspiration estimates against the water balance method, *J.*
796 *Hydrol.*, 538, 82-95, 2016a.

797 Liu, W.B., Wang, L., Chen, D.L., Tu, K., Ruan, C.Q., and Hu, Z.Y.: Large-scale circulation
798 classification and its links to observed precipitation in the eastern and central Tibetan Plateau,
33 / 62

799 Clim. Dyn., 46, 3481-3497, 2016b.

800 Liu, X.M., Yang, T., Hsu, K., Liu, C., and Sorooshian, S.: Evaluating the streamflow simulation
801 capability of PERSIANN-CDR daily rainfall products in two river basins on the Tibetan Plateau,
802 Hydrol. Earth Syst. Sci. Discuss., doi: 10.5194/hess-20160282, 2016.

803 Long, D., Shen, Y.J., Sun, A., Hong, Y., Longuevergne, L., Yang, Y.T., Li, B., and Chen, L.:
804 Drought and flood monitoring for a large karst plateau in Southwest China using extended
805 GRACE data, Remote Sens. Environ., 155, 145-160, 2014.

806 Lucchesi, R.: File specification for MERRA products, GMAO Office Note No.1 (version 2.3), 82
807 pp, available from http://gmao.gsfc.nasa.gov/pubs/office_notes, 2012.

808 Ma, N., Szilagyi, J., Niu, G.Y., Zhang, Y.S., Zhang, T., Wang, B.B., and Wu, Y.H.: Evaporation
809 variability of Nam Co Lake in the Tibetan Plateau and its role in recent rapid lake expansion, J.
810 Hydrol., 537, 27-35, 2016.

811 Ma, N., Zhang, Y.S., Guo, Y.H., Gao, H.F., Zhang, H.B., and Wang, Y.F.: Environmental and
812 biophysical controls on the evapotranspiration over the highest alpine steppe, J. Hydrol., 529,
813 980-992, 2015.

814 Mamat, A., Halik, W., and Yang, X.: The climatic changes of Qarqan river basin and its impact on
815 the runoff, Xinjiang Agric. Sci., 47 (5), 996-1001, 2010 (in Chinese).

816 Mansur, S. and Ajinisa, T.: An analysis of water resources and its hydrological characteristics of
817 Yarkend River Valley, J. Xinjiang Norm. Univ. (Nat. Sci. Ed.), 24(1), 74-78, 2005 (in Chinese).

818 McVicar, T.R., Roderick, M., Donohue, R.J., Li, L.T., Van Niel, T.G., Thomas, A., Grieser, J.,
819 Jhajharia, D., Himri, Y., Mahowald, N.M., Mescherskaya, A.V., Kruger, A.C., Rehman, S., and
820 Dinpashoh, Y.: Global review and synthesis of trends in observed terrestrial near-surface wind
821 speeds: implications for evaporation, J. Hydrol., 416-417, 182-205, 2012.

822 Miralles, D.G., De Jeu, R.A.M., Gash, J.H., Holmes, T.R.H., and Dolman, A.J.: Magnitude and
823 variability of land evaporation and its components at the global scale, Hydrol. Earth Syst. Sci., 15,
824 967-981, 2011.

825 Miralles, D.G., Gash, J.H., Holmes, T.R.H., de Jeu, R.A.M., and Dolman, A.J.: Global canopy
826 interception from satellite observations, J. Geophys. Res., 115, D16122, 2010.

827 Neckel, N., Kropáčková, J., Bolch, T., and Hochschild, V.: Glacier mass changes on the Tibetan
828 Plateau 2003-2009 derived from ICESat laser altimetry measurements, Environ. Res. Lett., 9,
34 / 62

829 014009(7pp), 2014.

830 Oliveira, P.T.S., Mearing, M.A., Moran, M.S., Goodrich, D.C., Wendland, E., and Gupta, H.V.:
831 Trends in water balance components across the Brazilian Cerrado, *Water Resour. Res.*, 50,
832 7100-7114, 2014.

833 Rodell, M., Houser, P.R., Jambor, U., Gottschalck, J., Mitchell, K., Meng, C.-J., Arsenault, K.,
834 Cosgrove, B., Radakovich, J., Bosilovich, M., Entin, J.K., Walker, P., Lohmann, D., and Toll, D.:
835 The global land data assimilation system, *B. Am. Meteorol. Soc.*, 85, 381-394, 2004.

836 Rui, H.: README Document for Global Land Data Assimilation System Version 2 (GLDAS-2)
837 Products, GES DISC, 2011.

838 Saji, N.H., Goswami, B.N., Vinayachandran, P.N., and Yamagata, T.: A dipole mode in the tropical
839 Indian Ocean, *Nature*, 401, 360-363, 1999.

840 Shen, M.G., Piao, S.L., Jeong, S., Zhou, L.M., Zeng, Z.Z., Ciais, P., Chen, D.L., Huang, M.T., Jin,
841 C.S., Li, L.Z.X., Li, Y., Myneni, R.B., Yang, K., Zhang, G.X., Zhang, Y.J., and Yao, T.D.:
842 Evaporative cooling over the Tibetan Plateau induced by vegetation growth, *Proc. Natl. Acad.*
843 *Sci. U. S.A.*, 112(30), 9299-9304, 2015.

844 Shi, Y.F., Shen, Y.P., Li, D.L., Zhang, G.W., Ding, Y.J., Hu, R.J., and Kang, E.S.: Discussion on
845 the present climate change from Warm2dry to Warm2wet in northwest China, *Quat. Sci.*, 23(2),
846 152-164, 2003 (in Chinese).

847 Shepard, D.S.: Computer mapping: the SYMAP interpolation algorithm. *Spatial Statistics and*
848 *Models*, G.L. Gaile and C.J. Willmott, Eds., D. Reidel, 133-145, 1984.

849 Sun, B., Mao, W., Feng, Y., Chang, T., Zhang, L., and Zhao, L.: Study on the change of air
850 temperature, precipitation and runoff volume in the Yarkant River basin, *Arid Zone Res.*, 23(2),
851 203-209, 2006 (in Chinese).

852 Takala, M., Luojus, K., Pulliainen, J., Derksen, C., Lemmetyinen, J., Kärnä J.-P., Koskinen, J., and
853 Bojkov, B.: Estimating northern hemisphere snow water equivalent for climate research through
854 assimilation of spaceborne radiometer data and ground-based measurements, *Remote*
855 *Sens. Environ.*, 115 (12), 3517-3529, 2011.

856 Tapley, B.D., Bettadpur, S., Watkins, M., and Rameisberger, C.: The gravity recovery and climate

857 experiment: mission overview and early results, *Geophys. Res. Lett.*, 31, L09607, 2004.

858 Tian, L., Yao, T., MacClune, K., White, J.W.C., Schilla, A., Vaughn, B., Vachon, R., and
859 Ichiyanagi, K.: Stable isotopic variations in west China: a consideration of moisture sources, *J.*
860 *Geophys. Res. Atmos.*, 112, D10112, 2007.

861 Tucker, C.J., Pinzon, J.E., Brown, M.E., Slayback, D., Pak, E.W., Mahoney, R., Vermote, E., and
862 El Saleous, N.: An extended AVHRR 8 km NDVI data set compatible with MODIS and SPOT
863 vegetation NDVI data, *Int. J. Remote Sens.*, 26(20), 4485-4498, 2005.

864 von Storch, H.: Misuses of statistical analysis in climate research, In *Analysis of Climate*
865 *Variability: Applications of Statistical Techniques*, Springer-Verlag: Berlin, 11-26, 1995.

866 Wang, A. and Zeng, X.: Evaluation of multireanalysis products within site observations over the
867 Tibetan Plateau, *J. Geophys. Res.*, 117, D05102, 2012.

868 Wang, L., Sun, L.T., Shrestha, M., Li, X.P., Liu, W.B., Zhou, J., Yang, K., Lu, H., and Chen, D.L.:
869 Improving snow process modeling with satellite-based estimation of
870 near-surface-air-temperature lapse rate, *J. Geophys. Res. Atmos.*, 121, 12005-12030, 2016.

871 Xia, Y., Mitchell, K., Ek, M., Cosgrove, B., Sheffield, J., Luo, L., Alonge, C., Wei, H., Meng, J.,
872 Livneh, B., and Duang, Q.: Continental-scale water and energy flux analysis and validation for
873 North American Land Data Assimilation System project phase 2 (NLDAS-2): 2. Validation of
874 model-simulated streamflow, *J. Geophys. Res. Atmos.*, 117(D3), D03110, 2012.

875 Xiang, L., Wang, H., Steffen, H., Wu, P., Jia, L., Jiang, L., and Shen, Q.: Groundwater storage
876 changes in the Tibetan Plateau and adjacent areas revealed from GRACE satellite gravity data,
877 *Earth Planet. Sci. Lett.*, 449, 228-239, 2016.

878 Xu, L.: The land surface water and energy budgets over the Tibetan Plateau, Available from
879 Nature Precedings < <http://hdl.handle.net/10101/npre.2011.5587.1>>, 2011.

880 Xue, B.L., Wang, L., Yang, K., Tian, L., Qin, J., Chen, Y., Zhao, L., Ma, Y., Koike, T., Hu, Z., and
881 Li, X.P.: Modeling the land surface water and energy cycle of a mesoscale watershed in the
882 central Tibetan Plateau with a distributed hydrological model, *J. Geophys. Res. Atmos.*, 118,
883 8857-8868, 2013.

884 Yao, Z., Duan, R., and Liu, Z.: Changes in precipitation and air temperature and its impacts on
885 runoff in the Nujiang River basins. *Resour. Sci.* 34(2), 202-210, 2012 (in Chinese)

886 Yang, K., Qin, J., Zhao, L., Chen, Y.Y., Tang, W.J., Han, M.L., Lazhu, Chen, Z.Q., Lv, N., Ding,
36 / 62

887 B.H., Wu, H., and Lin, C.G.: A multi-scale soil moisture and freeze-thaw monitoring network
888 on the third pole, *Bull. Am. Meteorol. Soc.*, 94,1907-1916, 2013.

889 Yang, K., Wu, H., Qin, J., Lin, C.G., Tang, W.J., and Chen, Y.Y.: Recent climate changes over the
890 Tibetan Plateau and their impacts on energy and water cycle: a review, *Glob. Planet Change*,
891 112, 79-91, 2014.

892 Yao, T.D., Thompson, L., Yang, W., Yu, W.S., Gao, Y., Guo, X.J., Yang, X.X., Duan, K.Q., Zhao,
893 H.B., Xu, B.Q., Pu, J.C., Lu, A.X., Xiang, Y., Kattel, D.B., and Joswiak, D.: Different glacier
894 status with atmospheric circulations in Tibetan Plateau and surroundings, *Nat. Clim. Change*, 2,
895 1-5, 2012.

896 Yao, Y.J., Zhao, S.H., Zhang, Y.H., Jia, K., and Liu, M.: Spatial and decadal variations in potential
897 evapotranspiration of China based on reanalysis datasets during 1982-2010, *Atmosphere*, 5,
898 737-754, 2014.

899 Yin, G., Hu, Z.Y., Chen, X., and Tiyyip, T.: Vegetation dynamics and its response to climate change
900 in Central Asia, *J. Arid Land*, 8, 375, 2016.

901 Yu, J., Zhang, G., Yao, T., Xie, H., Zhang, H., Ke, C., and Yao, R.: Developing daily cloud-free
902 snow composite products from MODIS Terra-Aqua and IMS for the Tibetan Plateau, *IEEE*
903 *Trans. Geosci. Remote Sens.*, 54(4), 2171-2180, 2015.

904 Yue, S., Pilon, P., Phinney, B., Cavadias, G.: The influence of autocorrelation on the ability to
905 detect trend in hydrological series, *Hydrol. Process.*, 16(9), 1807-1829, 2002.

906 Zhang, D., Liu, X., Zhang, Q., Liang, K., and Liu, C.: Investigation of factors affecting
907 inter-annual variability of evapotranspiration and streamflow under different climate conditions.
908 *J. Hydrol.*, doi:10.1016/j.jhydrol.2016.10.047, 2016.

909 Zhang, G., Xie, H., Yao, T., Liang, T., and Kang, S.: Snow cover dynamics of four lake basins
910 over Tibetan Plateau using time series MODIS data (2001-2100), *Water Resour. Res.*, 48(10),
911 W10529, 2012.

912 Zhang, K., Kimball, J.S., Nemani, R.R., and Running, S.W.: A continuous satellite-derived global
913 record of land surface evapotranspiration from 1983 to 2006, *Water Resour. Res.*, 46(9),
914 W09522, 2010.

915 Zhang, L., Su, F., Yang, D., Hao, Z., and Tong, K.: Discharge regime and simulation for the
916 upstream of major rivers over Tibetan Plateau, *J. Geophys. Res. Atmos.*, 118(15), 8500-8518,
37 / 62

917 2013.

918 Zhang, Q., Li, J., Singh, V., and Xu, C.: Copula-based spatial-temporal patterns of precipitation
919 extremes in China, *Int. J. Climatol.*, 33, 1140-1152, 2013.

920 Zhang, X., Tang, Q., Pan, M., and Tang, Y.: A long-term land surface hydrologic fluxes and states
921 dataset for China, *J. Hydrometeorol.*, 15, 2067-2084, 2014.

922 Zhang, Y., Peña-Arancibia, J.L., McVicar, T.R., Chiew, F.H.S., Vaze, J., Liu, C.M., Lu, X.J.,
923 Zheng, H.X., Wang, Y.P., Liu, Y.Y., Miralles, D.G., and Pan, M.: Multi-decadal trends in global
924 terrestrial evapotranspiration and its components, *Scientific Reports*, 6, 19124, 2016.

925 Zhang, Y., Liu, C., Tang, Y., and Yang, Y.: Trend in pan evaporation and reference and actual
926 evapotranspiration across the Tibetan Plateau, *J. Geophys. Res.*, 112, D12110, 2007.

927 Zhou, C., Jia, S., Yan, H., and Yang, G.: Changing trend of water resources in Qinghai Province
928 from 1956 to 2000, *J. Glaciol. Geocryol.*, 27(3), 432-437, 2005 (in Chinese).

929 Zhou, J., Wang, L., Zhang, Y.S., Guo, Y.H., Li, X.P., and Liu, W.B.: Exploring the water storage
930 changes in the largest lake (Selin Co) over the Tibetan Plateau during 2003-2012 from a
931 basin-wide hydrological modeling., *Water Resour. Res.*, 51, 8060-8086, 2015.

932 Zhou, S.Q., Kang, S., Chen, F., and Joswiak, D.R.: Water balance observations reveal significant
933 subsurface water seepage from Lake Nam Co., south-central Tibetan Plateau., *J. Hydrol.*, 491,
934 89-99, 2013.

935 Zhou, S.Q., Wang, Z., and Joswiak, D.R.: From precipitation to runoff: stable isotopic fractionation
936 effect of glacier melting on a catchment scale, *Hydrol. Process.*, 28(8), 3341-3349, 2014.

937 Zhu, Y., Chen, J., Chen, G.: Runoff variation and its impacting factors in the headwaters of the
938 Yangtze River in recent 32 years, *J. Yangtze River Sci. Res. Inst.*, 28(6), 1-4, 2011 (in Chinese).

939 ~~Table 1: Main features of the 18 used TP river basins. GA% and SC% represent the percentages of multiyear mean glacier cover and snow cover in each basin.~~
 940 ~~The glacier and snow cover data are extracted, respectively, from the Second Glacier Inventory Dataset of China and the daily TP snow cover dataset~~
 941 ~~(2005-2013).~~

942
 943
 944
 945
 946

Table 21: Overview of multi-source datasets applied in this study

Data category	Data source	Spatial resolution	Temporal resolution	Available period used	Reference
Runoff (Q)	Observed, National Hydrology Almanac of China	—	Daily	1982-2011	—
	VIC_IGSNRR simulated	0.25°	Daily	1982-2011	Zhang et al. (2014)
Precipitation (P)	Observed, CMA	0.5°	Monthly	1982-2011	—
	TRMM 3B43 V7	0.25°	Monthly	2000-2011	Huffman et al. (2012)
	IGSNRR forcing	0.25°	Daily	1982-2011	Zhang et al. (2014)
Temperature (Temp.)	Observed, CMA	0.5°	Monthly	2000-2011	—
Terrestrial storage change (ΔS)	GRACE-CSR	Approx.300-400 km	Monthly	2002-2011	Tapley et al. (2004)
	GRACE-GFZ	Approx.300-400 km	Monthly	2002-2011	Tapley et al. (2004)
	GRACE-JPL	Approx.300-400 km	Monthly	2002-2011	Tapley et al. (2004)
Potential evaporation (PET)	CRU	0.5°	Monthly	1982-2011	Harris et al. (2013)
Actual evaporation (ET)	MTE_E	0.5°	Monthly	1982-2011	Jung et al. (2010)
	VIC_E	0.25°	Daily	1982-2011	Zhang et al. (2014)
	GLEAM_E	0.25°	Daily	1982-2011	Miralles et al. (2011)
	PML_E	0.5°	Monthly	1982-2011	Zhang Y et al. (2016)
	Zhang_E	8 km	Monthly	1983-2006	Zhang et al. (2010)
	GNoah_E	1.0°	3 hourly	1982-2011	Rui (2011)

NDVI	GIMMS NDVI dataset	8 km	15 daily	1982-2011	Tucker et al. (2005)
LAI	GLASS LAI Product	0.05°	8 daily	1982-2011	Liang and Xiao (2012)
Snow Cover	TP Snow composite Products	500 m	Daily	2005-2013	Zhang et al. (2012)
SWE	VIC_IGSNRR simulated	0.25°	Daily	1982-2011	Zhang et al. (2014)
	GlobSnow-2 Product	25 km	Daily	1982-2011	Takala et al. (2011)
<u>Glacier Area</u>	<u>the Second Glacier Inventory Dataset of China</u>	-	-	<u>2005</u>	<u>Guo et al. (2014)</u>

带格式的: 字体: 五号, 字体颜色: 自动设置

带格式的: 字体: 五号, 字体颜色: 自动设置

947 Table 12: Main features of the 18 used TP river basins used in this study. The precipitation and temperature statistics for each basin were calculated from the
948 observed
949 CMA datasets while the NDVI and LAI statistics were extracted from the GIMMS NDVI dataset and GLASS LAI product. The GA% and SC% represented the
950 percentages of multiyear-mean glacier cover and snow cover in each basin which were calculated. The glacier and snow cover data are extracted, respectively, from
951 the Second Glacier Inventory Dataset of China and the daily
952 TP snow cover dataset (2005-2013)-
953

<u>No.</u>	<u>Station</u>	<u>Altitude (m)</u>	<u>River name</u>	<u>Drainage area (km²)</u>	<u>Multiyear-mean (1982-2011) and basin-averaged parameters</u>						
					<u>Q (mm/yr)</u>	<u>Prec. (mm/yr)</u>	<u>Temp. (°C/yr)</u>	<u>NDVI</u>	<u>LAI</u>	<u>GA%</u>	<u>SC%</u>
<u>01</u>	<u>Kulukelangan</u>	<u>2000</u>	<u>Yerqiang</u>	<u>32880.00</u>	<u>158.60</u>	<u>128.34</u>	<u>-5.68</u>	<u>0.05</u>	<u>0.03</u>	<u>10.97</u>	<u>35.03</u>
<u>02</u>	<u>Tongguziluoke</u>	<u>1650</u>	<u>Yulongkashi</u>	<u>14575.00</u>	<u>151.56</u>	<u>134.04</u>	<u>-4.07</u>	<u>0.06</u>	<u>0.04</u>	<u>23.27</u>	<u>35.95</u>
<u>03</u>	<u>Numaitilangan</u>	<u>1880</u>	<u>Keliya</u>	<u>7358.00</u>	<u>103.18</u>	<u>137.14</u>	<u>-4.78</u>	<u>0.06</u>	<u>0.03</u>	<u>10.86</u>	<u>29.16</u>
<u>04</u>	<u>Zelingou</u>	<u>4282</u>	<u>Bayin</u>	<u>5544.00</u>	<u>41.42</u>	<u>340.68</u>	<u>-4.98</u>	<u>0.13</u>	<u>0.09</u>	<u>0.09</u>	<u>21.22</u>
<u>05</u>	<u>Gadatan</u>	<u>3823</u>	<u>Yellow</u>	<u>7893.00</u>	<u>200.95</u>	<u>566.01</u>	<u>-4.60</u>	<u>0.34</u>	<u>0.54</u>	<u>0.13</u>	<u>14.94</u>
<u>06</u>	<u>Xining</u>	<u>3225</u>	<u>Yellow</u>	<u>9022.00</u>	<u>99.90</u>	<u>503.74</u>	<u>0.97</u>	<u>0.36</u>	<u>0.70</u>	<u>0.00</u>	<u>10.06</u>
<u>07</u>	<u>Tongren</u>	<u>3697</u>	<u>Yellow</u>	<u>2832.00</u>	<u>149.36</u>	<u>533.25</u>	<u>-1.37</u>	<u>0.39</u>	<u>0.83</u>	<u>0.00</u>	<u>9.42</u>
<u>08</u>	<u>Tainaihai</u>	<u>2632</u>	<u>Yellow</u>	<u>121972.00</u>	<u>159.48</u>	<u>540.32</u>	<u>-2.40</u>	<u>0.34</u>	<u>0.72</u>	<u>0.09</u>	<u>15.89</u>
<u>09</u>	<u>Huangheyan</u>	<u>4491</u>	<u>Yellow</u>	<u>20930.00</u>	<u>31.18</u>	<u>386.42</u>	<u>-4.81</u>	<u>0.23</u>	<u>0.61</u>	<u>0.00</u>	<u>17.25</u>
<u>10</u>	<u>Jimai</u>	<u>4450</u>	<u>Yellow</u>	<u>45015.00</u>	<u>85.50</u>	<u>441.48</u>	<u>-4.16</u>	<u>0.26</u>	<u>0.52</u>	<u>0.00</u>	<u>20.05</u>

<u>11</u>	<u>Yajiang</u>	<u>2599</u>	<u>Yalong</u>	<u>67514.00</u>	<u>237.66</u>	<u>717.05</u>	<u>-0.23</u>	<u>0.43</u>	<u>0.80</u>	<u>0.15</u>	<u>18.36</u>
<u>12</u>	<u>Zhimenda</u>	<u>3540</u>	<u>Yangtze</u>	<u>137704.00</u>	<u>96.23</u>	<u>405.66</u>	<u>-4.83</u>	<u>0.20</u>	<u>0.26</u>	<u>0.96</u>	<u>17.87</u>
<u>13</u>	<u>Jiaoyuqiao</u>	<u>3000</u>	<u>Salween</u>	<u>72844.00</u>	<u>364.26</u>	<u>620.88</u>	<u>-1.89</u>	<u>0.29</u>	<u>0.44</u>	<u>2.02</u>	<u>23.73</u>
<u>14</u>	<u>Pangduo</u>	<u>5015</u>	<u>Brahmaputra</u>	<u>16459.00</u>	<u>348.31</u>	<u>544.59</u>	<u>-1.53</u>	<u>0.27</u>	<u>0.33</u>	<u>1.66</u>	<u>23.33</u>
<u>15</u>	<u>Tangjia</u>	<u>4982</u>	<u>Brahmaputra</u>	<u>20143.00</u>	<u>350.61</u>	<u>555.17</u>	<u>-1.89</u>	<u>0.27</u>	<u>0.34</u>	<u>1.39</u>	<u>21.83</u>
<u>16</u>	<u>Gongbuijiangda</u>	<u>4927</u>	<u>Brahmaputra</u>	<u>6417.00</u>	<u>586.96</u>	<u>692.06</u>	<u>-4.24</u>	<u>0.27</u>	<u>0.36</u>	<u>4.12</u>	<u>25.99</u>
<u>17</u>	<u>Nuxia</u>	<u>2910</u>	<u>Brahmaputra</u>	<u>191235.00</u>	<u>307.38</u>	<u>401.35</u>	<u>-0.73</u>	<u>0.22</u>	<u>0.25</u>	<u>1.90</u>	<u>13.50</u>
<u>18</u>	<u>Yangcun</u>	<u>3600</u>	<u>Brahmaputra</u>	<u>152701.00</u>	<u>163.25</u>	<u>349.91</u>	<u>-0.87</u>	<u>0.19</u>	<u>0.18</u>	<u>1.28</u>	<u>10.52</u>

954
955
956
957
958
959

Table 33: Contribution of glacier-melt to discharge in ~~eighteen~~ **18 TP** basins (“—” shows no glacier influences, “—*” shows the percentage is empirically estimated through the relation between glacier area ratio and glacier melt for basins in which the glacier melt contribution has been reported in the literatures)

Basin	Contributions of glacier-melt to discharge (%)	Reference
Kulukelangan	62.7 3	Mansur and Ajnisa (2005)
Tongguziluoke	64.9 9	Liu J et al. (2016)
Numaitilangan	71. <u>0</u>	Chen (1988)
Zelingou	—	—
Gadatan	—	—
Xining	—	—
Tongren	—	—
Tainaihai	0.8 9	Zhang et al. (2013)
Huangheyuan	—	—
Jimai	—	—

Yajiang	1.4 0	—*
Zhimenda	6.5 0	Zhang et al. (2013)
Jiaoyuqiao	4.8 0	Zhang et al. (2013)
Nuxia	11.6 0	Zhang et al. (2013)
Pangduo	10.1 3	—*
Tangjia	8.5 49	—*
Gongbujiangda	25.2 15	—*
Yangcun	7.8 1	—*

960
961
962
963
964
965

Table 4: Annual-averaged water storage changes (ΔS) in 18 TP basins derived from GRACE retrievals (2002-2013) from three different processing centers (CSR, GFZ and JPL)

Basin	Water storage Change (ΔS ,mm)		
	CSR	GFZ	JPL
<u>Kulukelangan</u>	<u>-0.16</u>	<u>-0.16</u>	<u>-0.00</u>
<u>Tongguziluoke</u>	<u>0.10</u>	<u>0.10</u>	<u>0.28</u>
<u>Numaitilangan</u>	<u>0.24</u>	<u>0.22</u>	<u>0.41</u>
<u>Zelingou</u>	<u>0.63</u>	<u>0.41</u>	<u>0.69</u>
<u>Gadatan</u>	<u>0.02</u>	<u>-0.24</u>	<u>-0.03</u>
<u>Xining</u>	<u>-0.08</u>	<u>-0.35</u>	<u>-0.14</u>
<u>Tongren</u>	<u>-0.13</u>	<u>-0.41</u>	<u>-0.21</u>
<u>Tainaihai</u>	<u>0.12</u>	<u>-0.16</u>	<u>0.10</u>
<u>Huangheyang</u>	<u>0.60</u>	<u>0.35</u>	<u>0.70</u>

- 带格式的: 行距: 多倍行距 2.5 字行
- 带格式表格
- 带格式的: 行距: 单倍行距
- 带格式的: 右
- 带格式的: 右, 行距: 单倍行距
- 带格式的: 右

<u>Jimai</u>	<u>0.41</u>	<u>0.15</u>	<u>0.48</u>
<u>Yajiang</u>	<u>-0.23</u>	<u>-0.50</u>	<u>-0.21</u>
<u>Zhimenda</u>	<u>0.57</u>	<u>0.38</u>	<u>0.78</u>
<u>Jiaoyuqiao</u>	<u>-1.00</u>	<u>-1.13</u>	<u>-0.79</u>
<u>Nuxia</u>	<u>-1.42</u>	<u>-1.44</u>	<u>-1.31</u>
<u>Pangduo</u>	<u>-1.21</u>	<u>-1.29</u>	<u>-1.02</u>
<u>Tangjia</u>	<u>-1.40</u>	<u>-1.46</u>	<u>-1.24</u>
<u>Gongbujiangda</u>	<u>-1.61</u>	<u>-1.67</u>	<u>-1.47</u>
<u>Yangcun</u>	<u>-1.33</u>	<u>-1.34</u>	<u>-1.21</u>

966
967
968
969
970

Table 45: Nonparametric trends for different ET estimates during the period 1982-2006 detected by modified Mann-Kendall test, the bold number showed the detected trend is statistically significant at the 0.05 level

Basin	ET _{wb}	GLEAM_E	VIC_E	Zhang_E	PML_E	MET_E	GNoah_E
Kulukelangan	-0.09	0.09	0.18	–	0.03	-0.01	0.07
Tongguziluoke	-0.02	0.10	0.13	–	0.03	-0.08	0.19
Numaitilangan	0.04	0.10	0.14	–	0.14	-0.10	0.22
Zelingou	0.13	0.23	0.11	0.09	0.04	0.06	0.02
Gadatan	-0.09	0.25	0.070	-0.10	-0.01	0.06	-0.07
Xining	-0.06	0.54	0.01	-0.08	0.01	0.02	-0.06
Tongren	-0.06	0.34	-0.15	-0.17	0.07	0.02	0.13
Tainaihai	0.06	0.28	-0.03	-0.11	0.04	0.05	0.04
Huangheyan	0.08	0.19	-0.01	-0.10	0.08	0.05	0.10

971	Jimai	-0.07	0.23	-0.01	-0.08	0.03	0.05	0.10
972	Yajiang	0.17	0.26	0.06	-0.21	-0.01	0.03	-0.02
973	Zhimenda	0.11	0.28	0.10	0.01	0.07	0.04	0.07
	Jiaoyuqiao	0.18	0.28	0.10	-0.11	0.05	0.05	0.07
974	Nuxia	-0.09	0.25	0.09	-0.10	0.12	0.04	0.10
	Pangduo	0.05	0.28	0.17	-0.07	0.07	0.07	0.11
	Tangjia	0.09	0.26	0.17	-0.09	0.20	0.06	0.12
975	Gongbujiangda	-0.26	0.12	0.13	-0.16	0.19	0.01	0.15
976	Yangcun	0.03	0.28	0.08	-0.06	0.10	0.04	0.09

977

978

979

980

981

982

983

984 **Figure captions:**

985 **Figure 1.** Map of river basins and hydrological gauging stations (green dots) over the
986 Tibetan Plateau (TP) used in this study. The grey shading shows the topography of TP
987 in meters above the sea level and the blue shading exhibits the glaciers distribution in
988 TP extracted from the Second Glacier Inventory Dataset of China.

989 **Figure 2.** Comparison of VIC_IGSNRR simulated and observed monthly runoff for
990 Tangnaihai and Panduo stations (a and b) as well as (c) basin-averaged monthly
991 TRMM, CMA gridded and IGSNRR forcing precipitations for the smallest basin
992 (Tongren station) over the period 1982-2011. (d) shows the comparison of TRMM
993 (blue) and IGSNRR forcing (red) precipitations against CMA gridded precipitation for
994 18 river basins over TP during the period 2000-2011.

995 **Figure 3.** Comparison of different ET products against the calculated ET through the
996 water balance method (ET_{wb}) at the monthly time scale for 18 TP basins during the
997 period 1983-2006. The boxplot of annual-monthly estimates of different ET products
998 for 18 TP basins are shown in (a) while the correlation coefficients and
999 root-mean-square-errors (RMSEs, mm/month) for each ET product relatively to ET_{wb}
1000 are exhibited in (b).

1001 **Figure 4.** General water and energy status (a. the perspective of Budyko framework)
1002 and their relationships with glacier (b) and vegetation (c and d) for eighteen TP river
1003 basins (1983-2006). The ET used in this figure is calculated from the bias-corrected
1004 water balance method.

1005 **Figure 5.** Seasonal cycles (1982-2011) of water budget components in westerlies-
1006 dominated (column 1), East Asian monsoon-dominated (columns 2-4) and Indian
1007 monsoon-dominated (columns 5-6) TP basins.

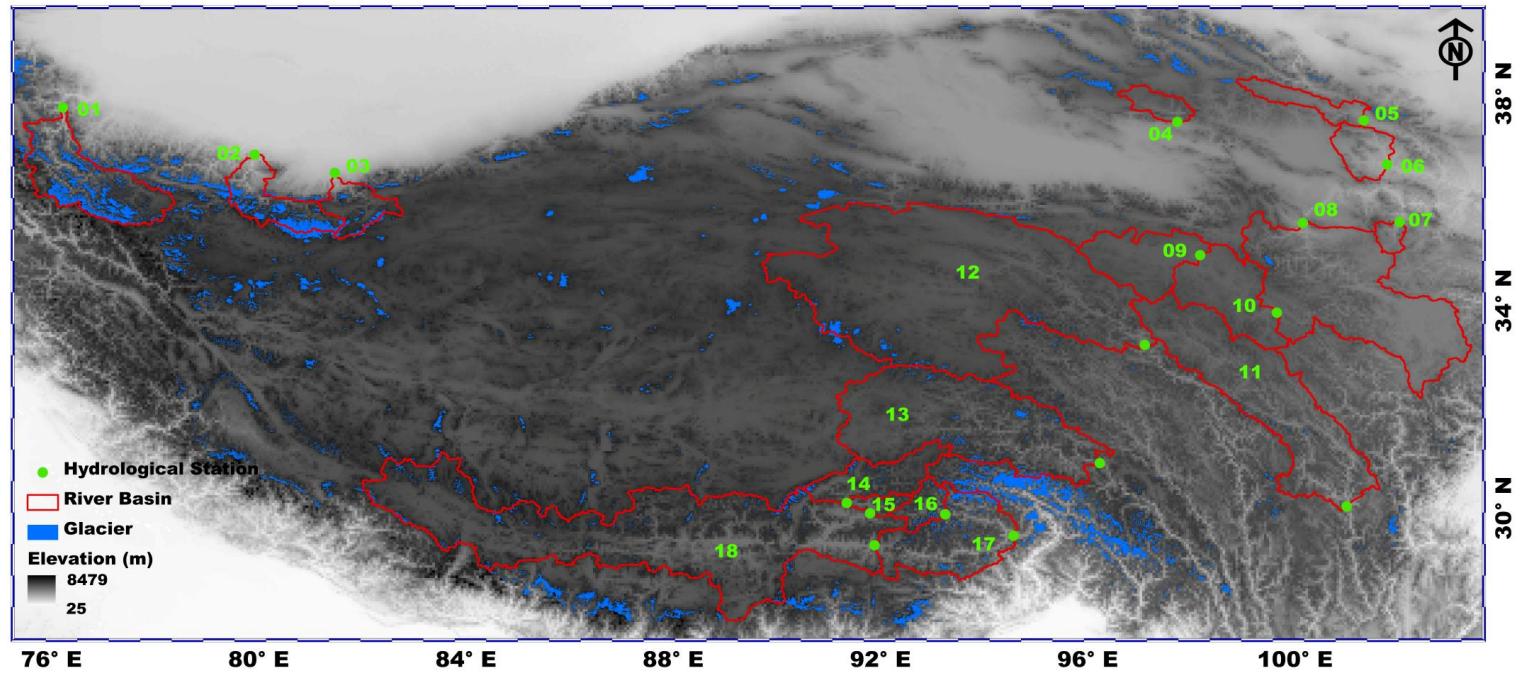
1008 **Figure 6.** Seasonal cycles (1982-2011) of air temperature and vegetation parameters
1009 in westerlies-dominated (column 1), East Asian monsoon-dominated (columns 2-4)
1010 and Indian monsoon-dominated (columns 5-6) TP basins.

1011 **Figure 7.** Seasonal cycles (1982-2011) of snow cover and snow water equivalent
1012 (SWE) in westerlies-dominated (column 1), East Asian monsoon-dominated (columns

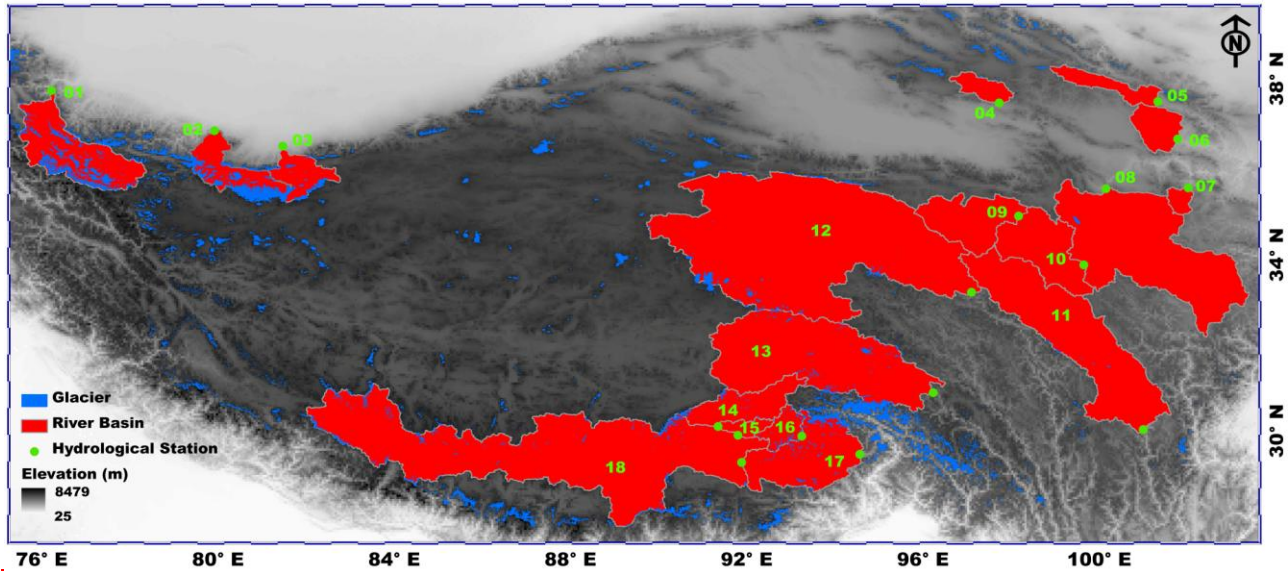
带格式的: 字体: 小四, 字体颜色:
文字 1

1013 2-4) and Indian monsoon-dominated (columns 5-6) TP basins. The snow cover was
1014 extracted from cloud free snow composite product during the period 2005-2013. It
1015 should also be noted that the GlobSnow data are not available for some basins.
1016 **Figure 8.** Sen's slopes of water budget components and vegetation parameters in
1017 westerlies-dominated TP basins during the period of 1982-2011. The double red stars
1018 showed that the trend was statistically significant at the 0.05 level.
1019 **Figure 9.** Linear and non-parametric trends of westerly, Indian monsoon and East
1020 Asian summer monsoon during the period 1982-2011 revealed prospectively by the
1021 Asian Zonal Circulation Index, Indian Ocean Dipole Mode Index and East Asian
1022 Summer Monsoon Index.
1023 **Figure 10.** Similar to Figure 8 but for East Asian monsoon-dominated TP basins. It
1024 should be noted that the GlobSnow data are not available for some basins. The double
1025 red stars showed that the trend was statistically significant at the 0.05 level.
1026 **Figure 11.** Similar to Figure 8 but for Indian monsoon-dominated TP basins. It should
1027 be noted that the GlobSnow data are not available for some basins. The double red
1028 stars showed that the trend was statistically significant at the 0.05 level.

1029 **Figure 1.** Map of river basins and hydrological gauging stations (green dots) over the Tibetan Plateau (TP) used in this study. The grey shading shows the
1030 topography of TP in meters above the sea level and the blue shading exhibits the glaciers distribution in TP extracted from the Second Glacier Inventory Dataset of
1031 China.

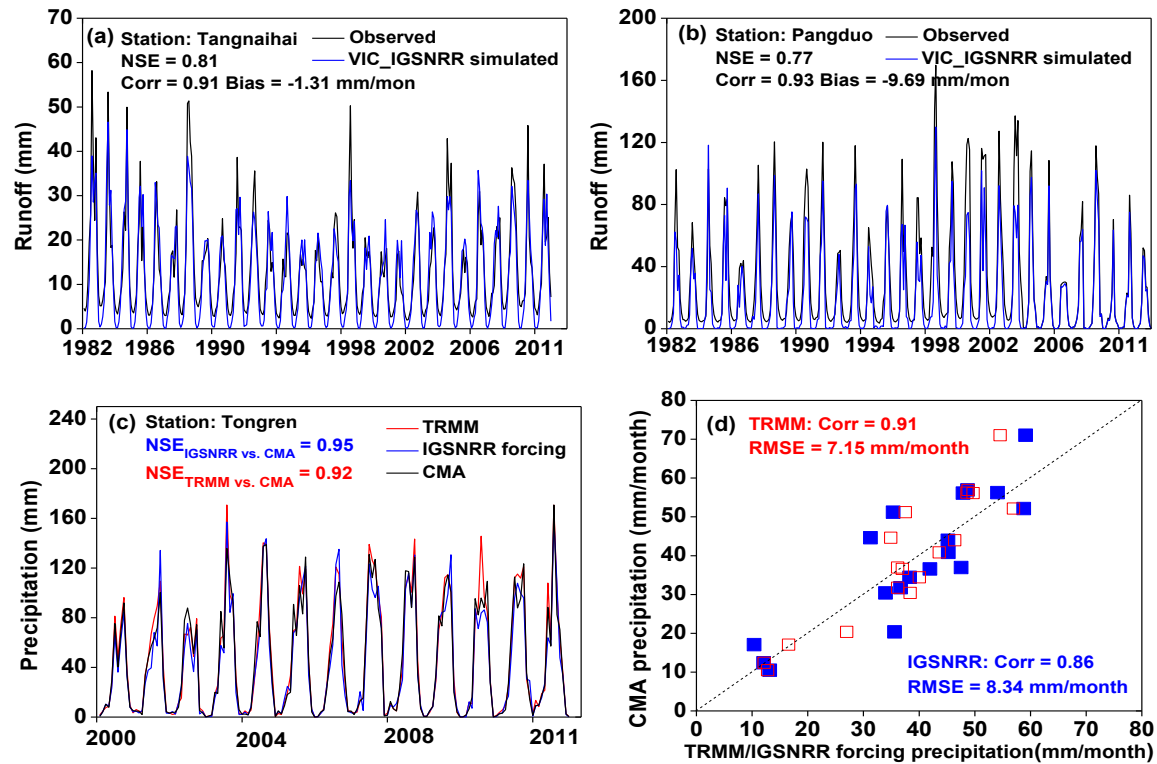


1032



1033
1034

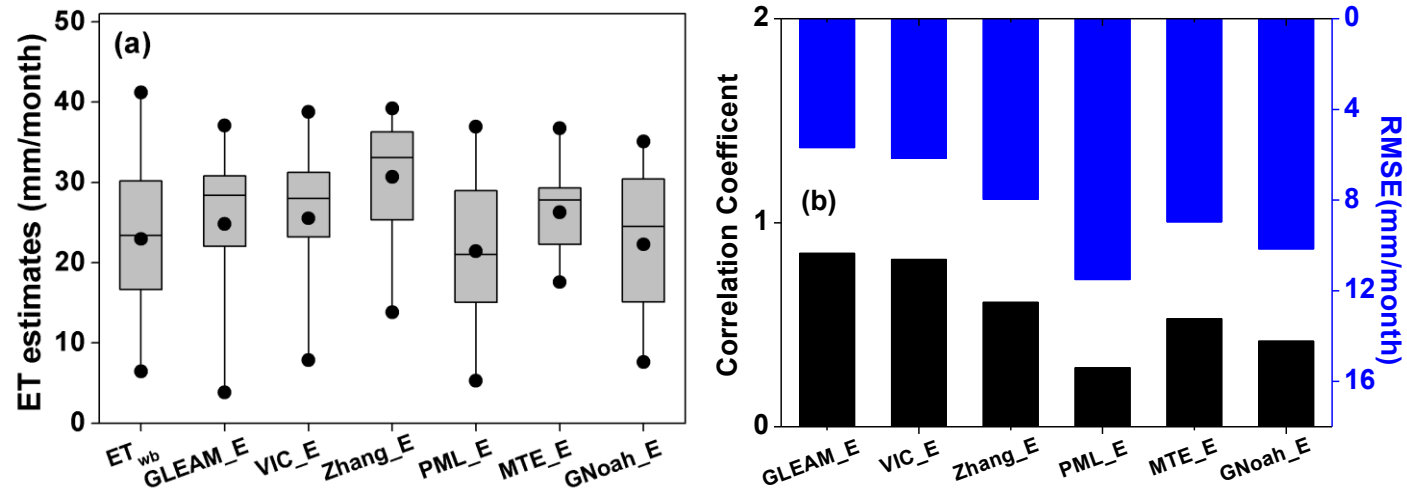
1035 **Figure 2.** Comparison of VIC_IGSNRR simulated and observed monthly runoff for Tangnaihai and Panduo stations (a and b) as well as (c) basin-averaged
 1036 monthly TRMM, CMA gridded and IGSNRR forcing precipitations for the smallest basin (Tongren station) over the period 1982-2011. (d) shows the comparison of
 1037 TRMM (blue) and IGSNRR forcing (red) precipitations against CMA gridded precipitation for 18 river basins over TP during the period 2000-2011.



1038

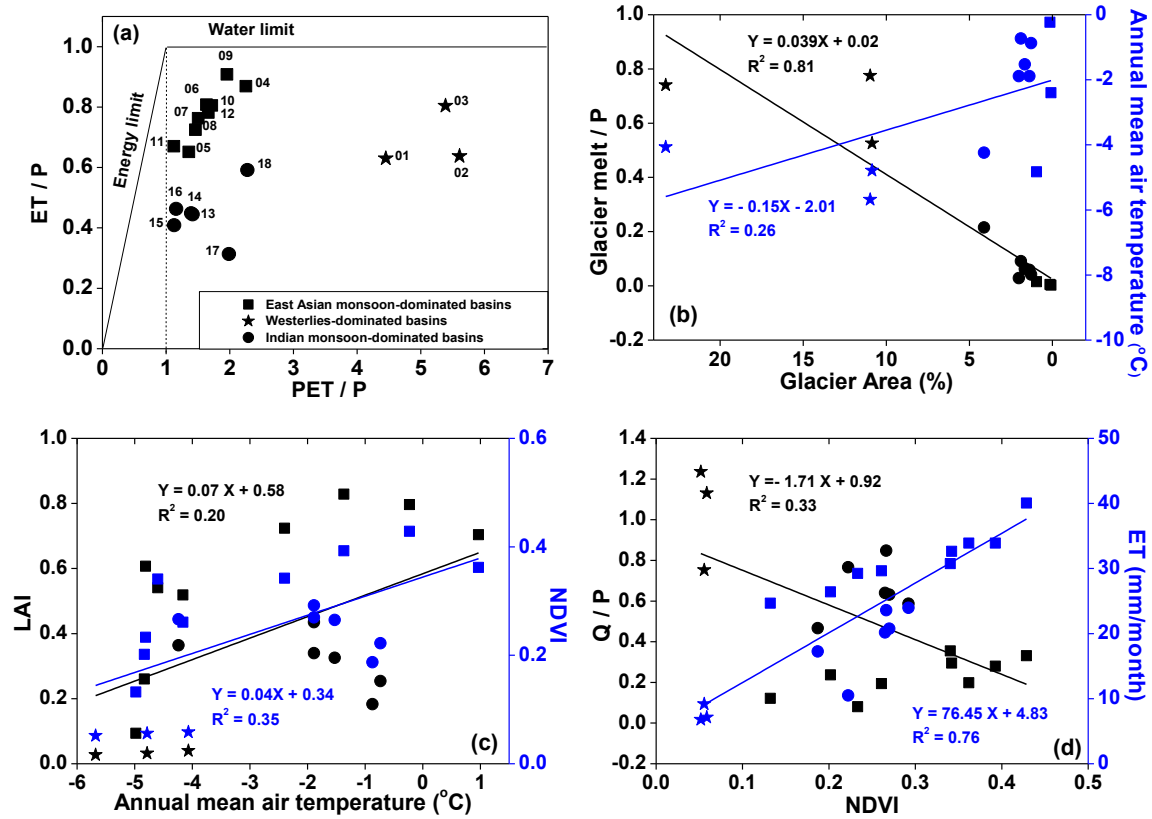
1039
1040

1041 **Figure 3.** Comparison of different ET products against the calculated ET through the water balance (ET_{wb}) at the monthly time scale for 18 river basins over the
 1042 Tibetan Plateau during the period 1983-2006. The boxplot of annual-monthly estimates of different ET products for 18 TP basins are shown in (a) while the
 1043 correlation coefficients and root-mean-square-errors (RMSEs, mm/month) for each ET product relatively to ET_{wb} are exhibited in (b).



1044
1045

1046 **Figure 4.** General water and energy status (a. the perspective of Budyko framework) and their relationships with glacier (b) and vegetation (c and d) for eighteen
 1047 TP river basins (1983-2006). The ET used in this figure is calculated from the bias-corrected water balance method.

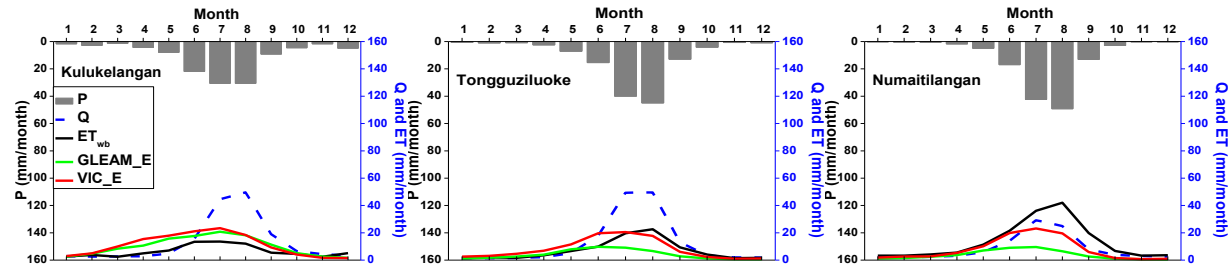


1048

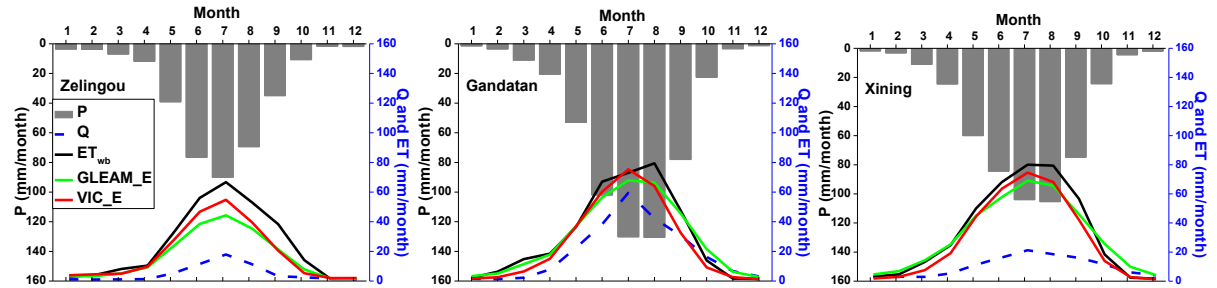
1049

1050 **Figure 5.** Seasonal cycles (1982–2011) of water budget components in westerlies-dominated (column 1), East Asian monsoon-dominated (columns 2–4) and Indian
 1051 monsoon-dominated (columns 5–6) TP basins.

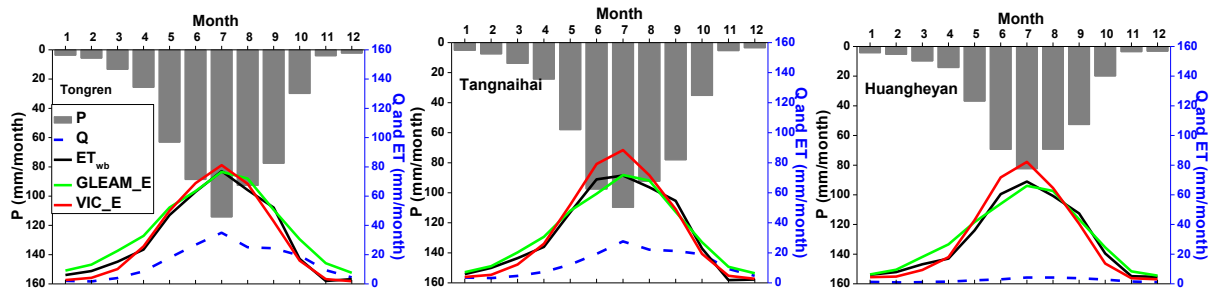
1052



1053



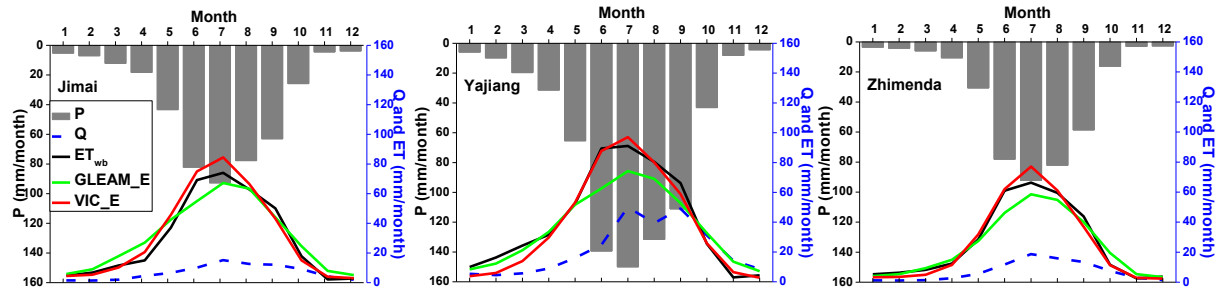
1054



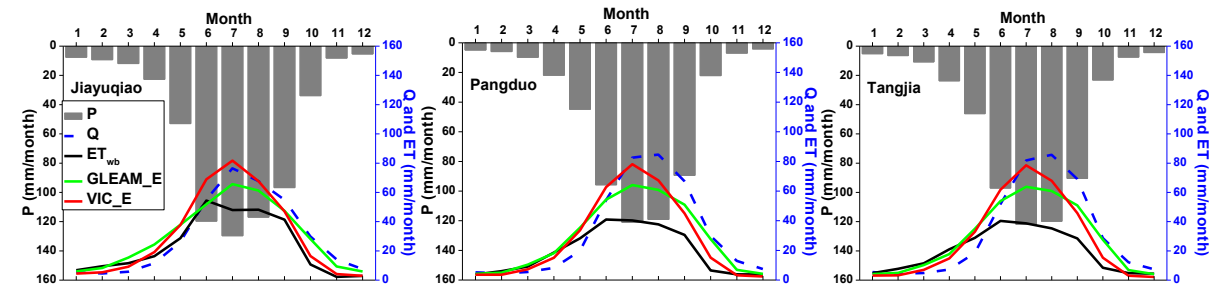
1055

Figure 5: (continued)

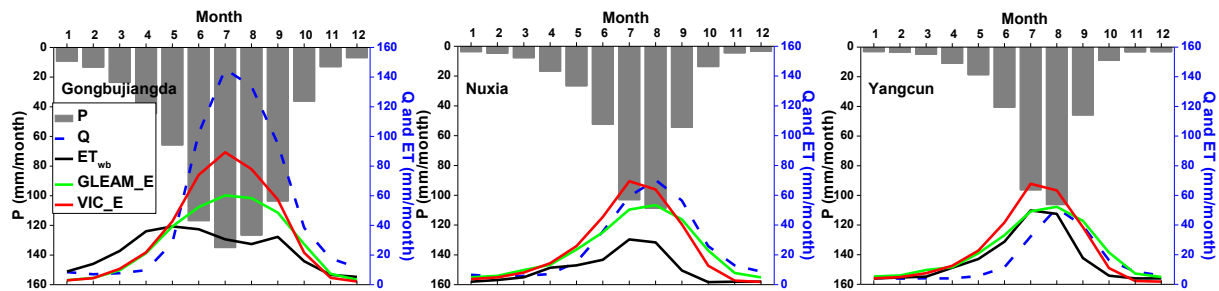
1056



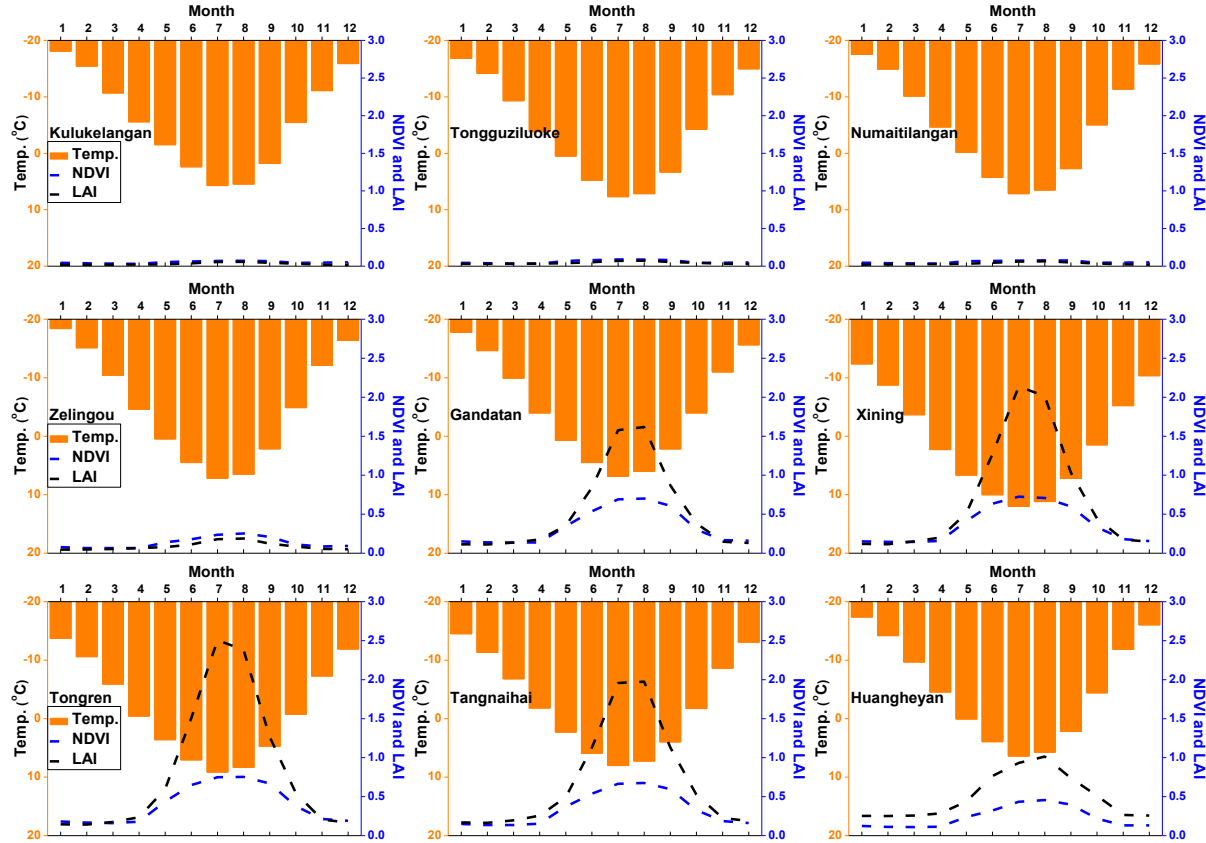
1057



1058



1059 **Figure 6.** Seasonal cycles (1982-2011) of air temperature and vegetation parameters in westerlies-dominated (column 1), East Asian monsoon-dominated (columns
 1060 2-4) and Indian monsoon-dominated (columns 5-6) TP basins.



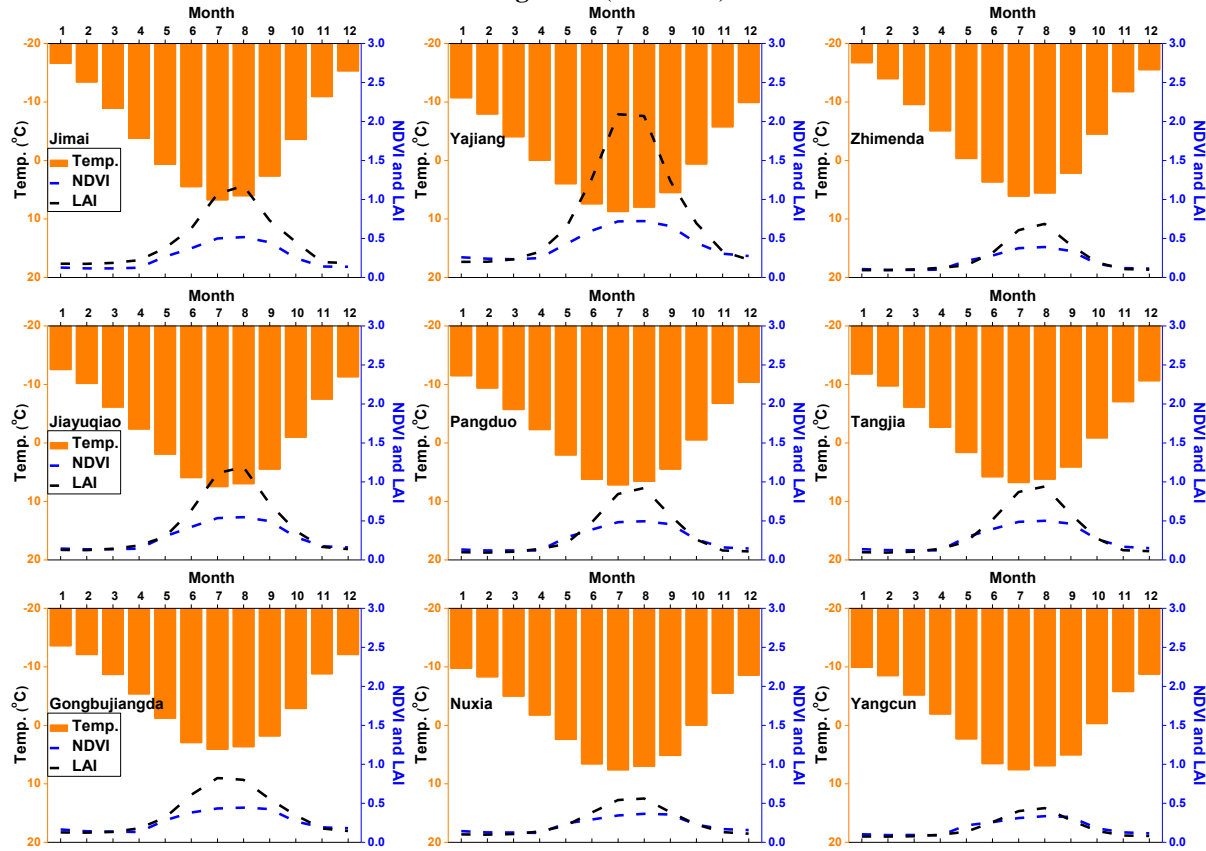
1061

1062

1063

1064

Figure 6: (continued)



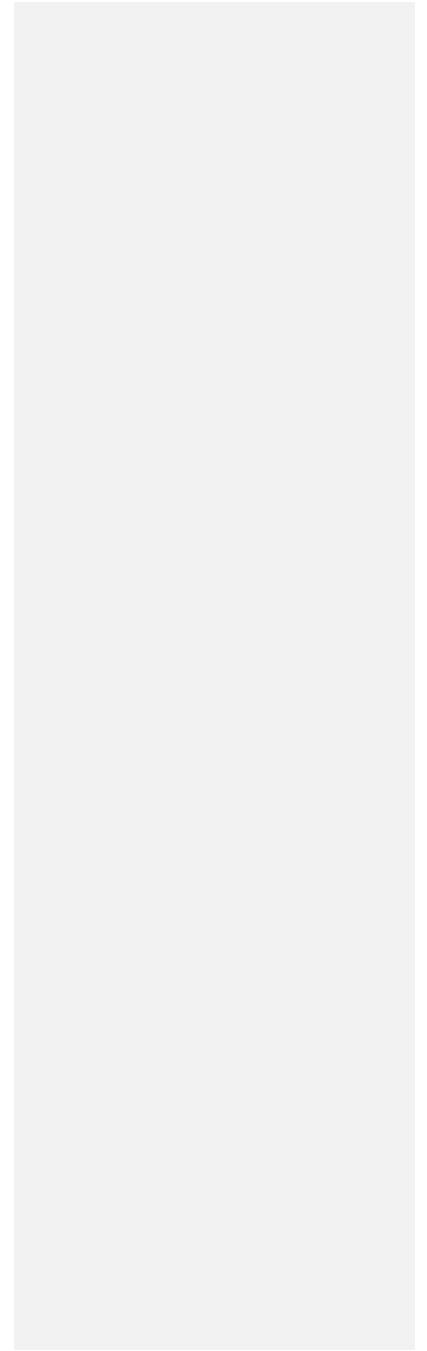
1065

1066

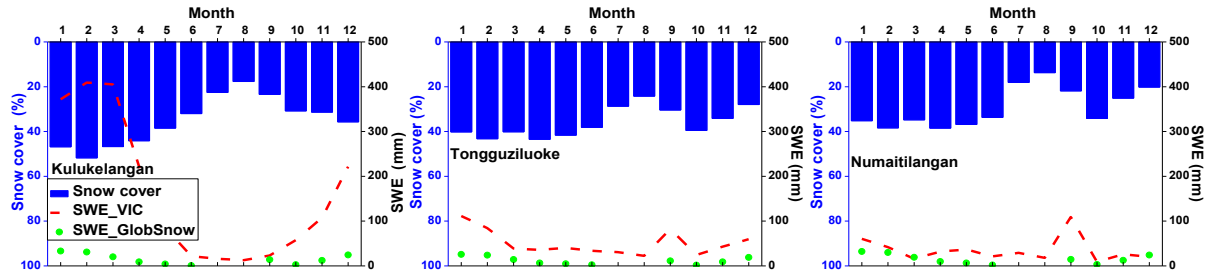
1067

1068

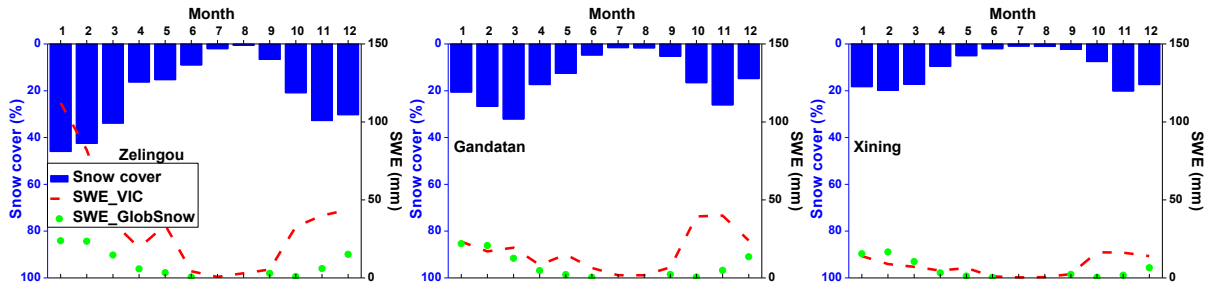
1069 **Figure 7.** Seasonal cycles (1982-2011) of snow cover and snow water equivalent (SWE) in westerlies-dominated (column 1), East Asian monsoon- dominated
1070 (columns 2-4) and Indian monsoon-dominated (columns 5-6) TP basins. The snow cover was extracted from cloud free snow composite product during the period
1071 2005-2013. It should also be noted that the GlobSnow data are not available for some basins.
1072



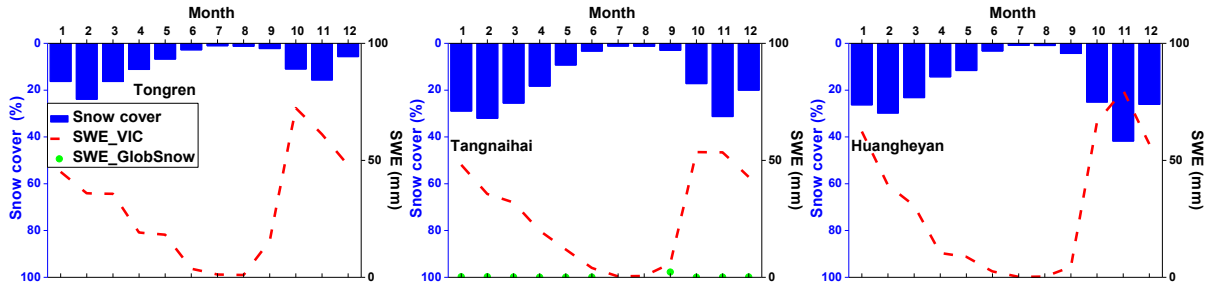
1073



1074



1075

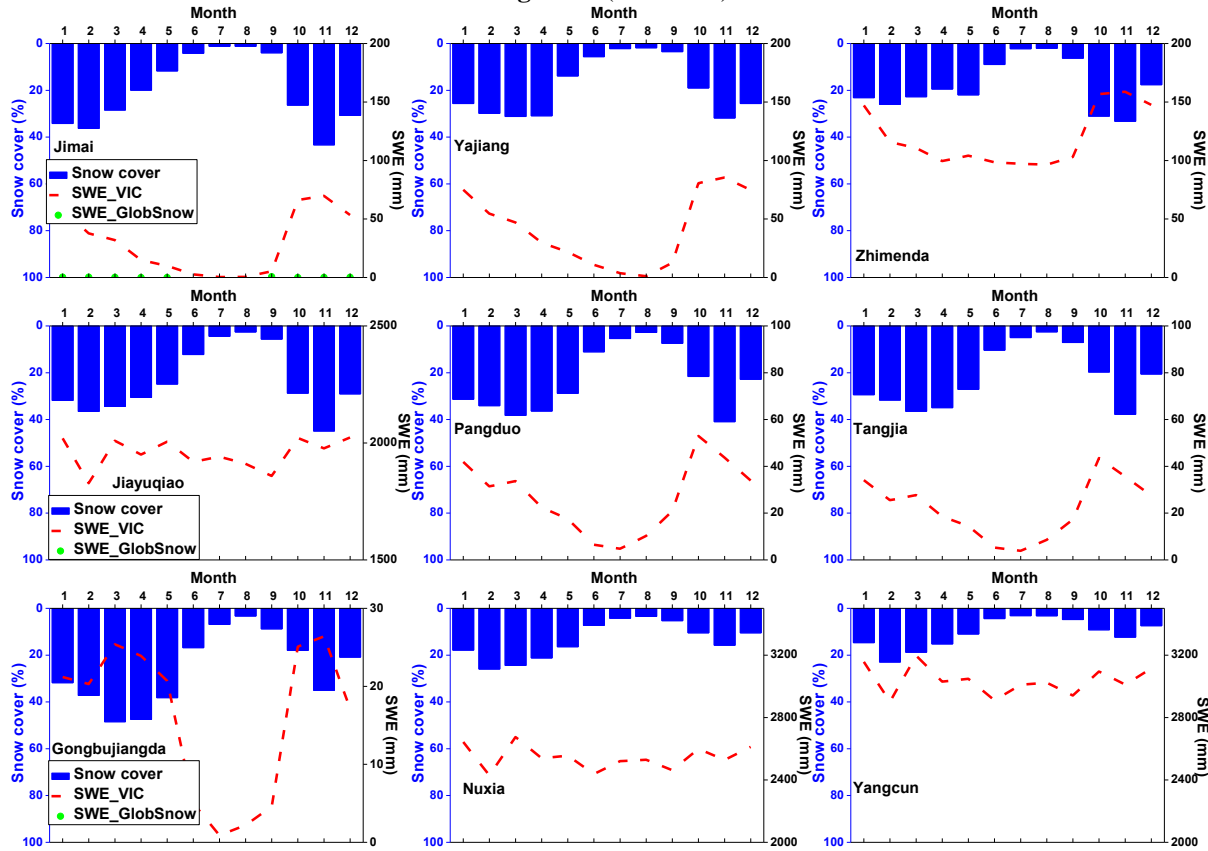


1076

1077

1078

Figure 7: (continued)



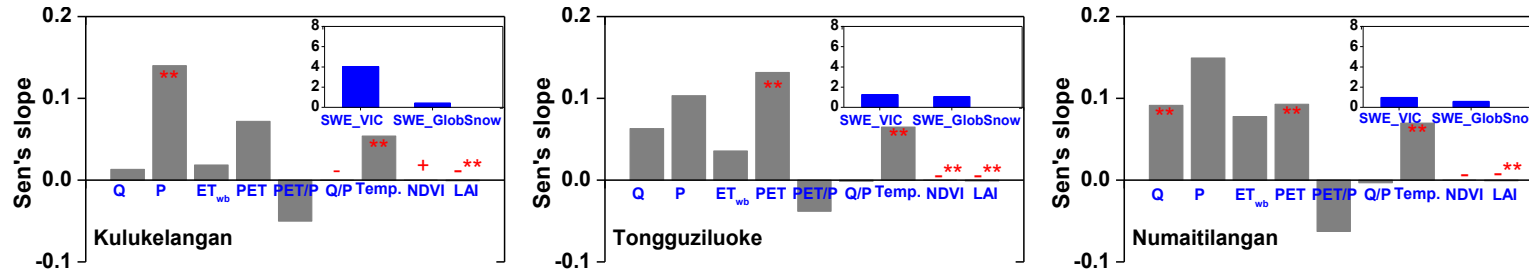
1079

1080

1081

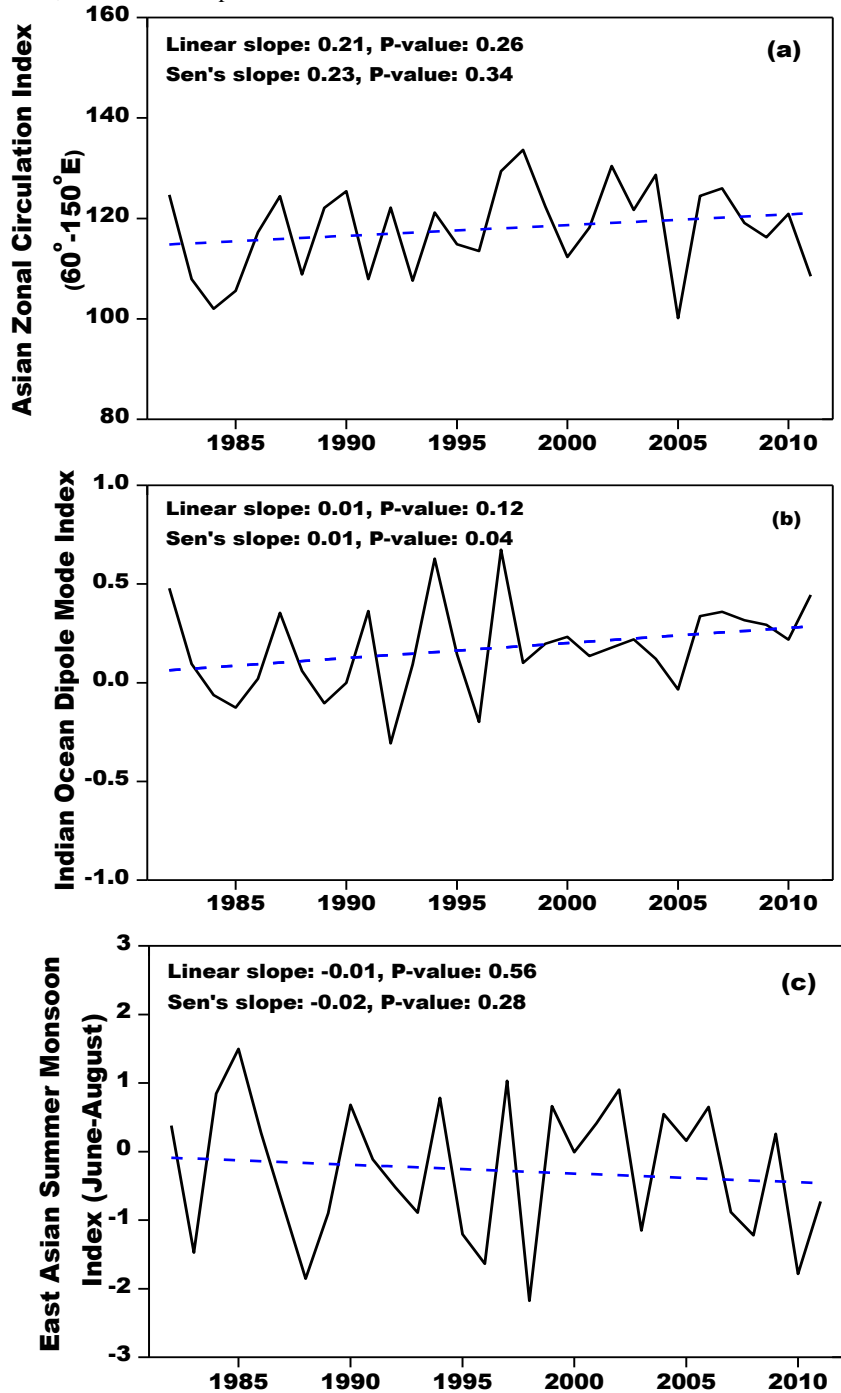
1082

1083 **Figure 8.** Sen's slopes of water budget components and vegetation parameters in westerlies-dominated TP basins during the period of 1982-2011. The double red
 1084 stars showed that the trend was statistically significant at the 0.05 level.



1085
 1086

1087 **Figure 9.** Linear and non-parametric trends of westerly, Indian monsoon and East Asian summer
 1088 monsoon during the period 1982-2011 revealed prospectively by the Asian Zonal Circulation
 1089 Index, Indian Ocean Dipole Mode Index and East Asian Summer Monsoon Index.

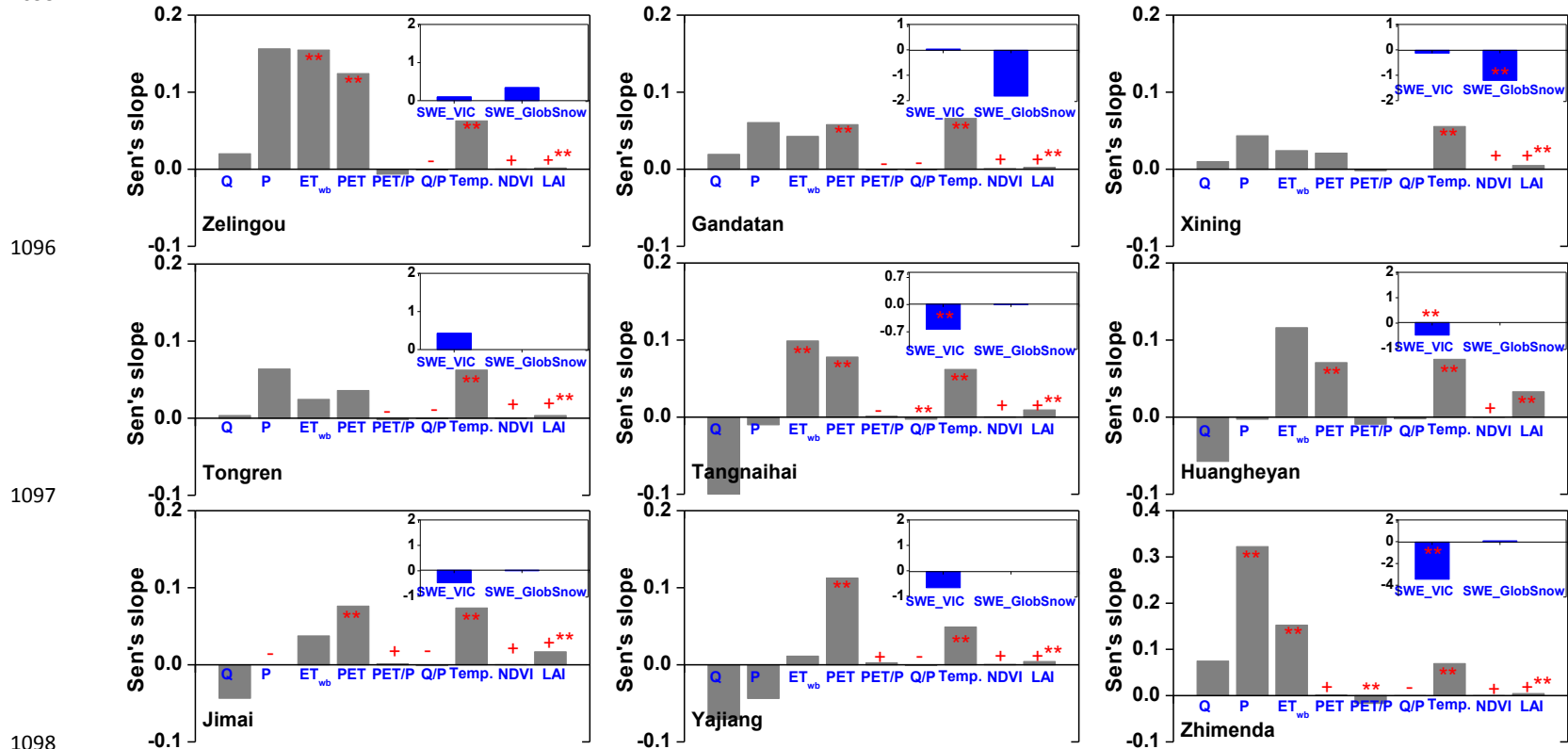


1090

1091

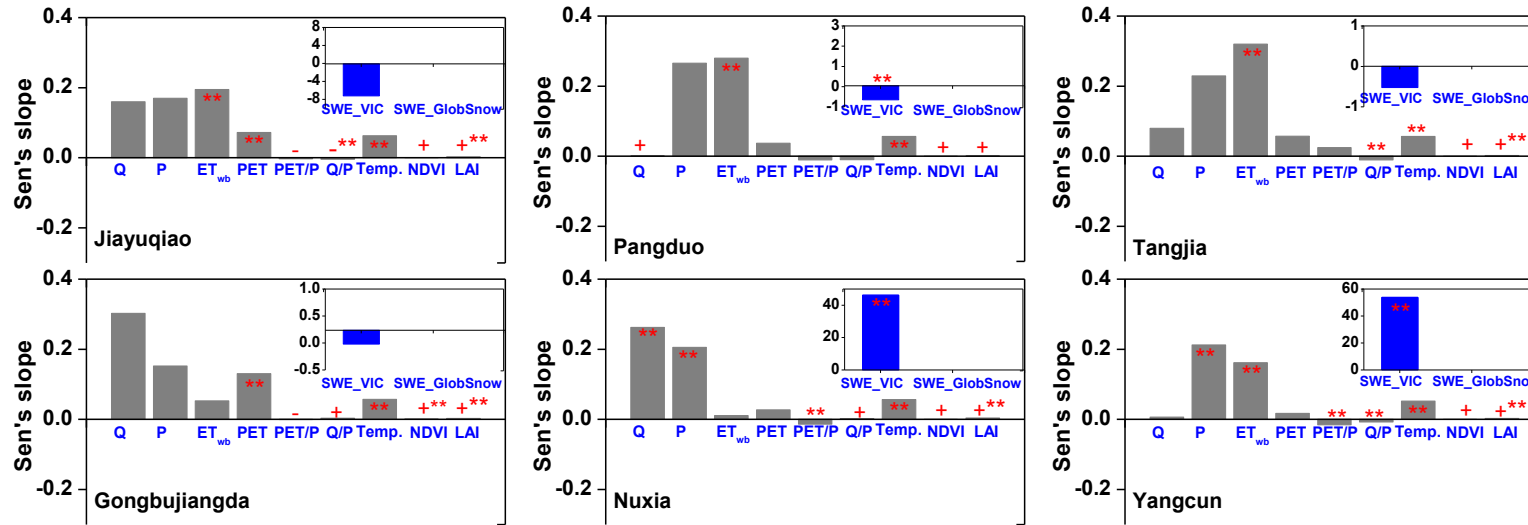
1092

1093 **Figure 10.** Similar to Figure 8 but for East Asian monsoon-dominated TP basins. It should be noted that the GlobSnow data are not available for some basins. The
 1094 double red stars showed that the trend was statistically significant at the 0.05 level.
 1095



1101 **Figure 11.** Similar to Figure 8 but for Indian monsoon-dominated TP basins. It should be noted that the GlobSnow data are not available for some basins. The
 1102 double red stars showed that the trend was statistically significant at the 0.05 level.
 1103

1104



1105